



**Politecnico
di Torino**

Department of Environment, Land and Infrastructure Engineering (DIATI)

Master of Science in Environmental and Land Engineering

**Microplastic Contamination in Rainwater:
A Case Study from S.A.S.S.O Monitoring Station
(Valle d'Aosta, Italy)**

Supervisor: **Professor. Paola Marini**

Co-supervisor: **Alireza Vejdaniwahid**

Candidate: **Meisam Afshari**

Academic Year: 2025-2026

March 2026

Abstract

Today, microplastic pollution has drawn global attention. Although many studies have recently been conducted on this topic, most have focused on marine environments. To better understand the distribution of microplastics, remote regions must also be investigated. Rainfall collection is an appropriate method to assess potential atmospheric microplastic contamination. However, in terms of methodologies and protocols, the process of MP investigation and identification of MP on rainwater samples is unclear. In this study, 27 rainfall samples were collected from Valle d'Aosta, a remote region. Preparation procedures were conducted on samples, for instance digestion of organic materials. After filtration, the filters were scanned, and their exact coordinates on the filter were recorded under a digital microscope to identify suspected MP fibres based on visual characteristics. Next, the selected fibres were tracked and identified by Raman.

The concentration of MP fibres varied across samples, ranging from 11 to 262, of which 65% could be identified by Raman spectroscopy. The results showed that PET was the most abundant polymer. The MP fibres were smaller than 1000 micrometres. In addition, black and white fibres were the most prevalent colours within the samples.

Keywords: Valle d'Aosta Microplastic, Raman spectroscopy, Rainwater, PET, Digital microscope 3D, contamination

"Dedicated to the brave souls of my fellow countrymen who fell for freedom.

A small token of remembrance for those who will never be forgotten."

3. March.2026

تقدیم به روح‌های شجاع هم‌وطنانم که در راه آزادی جان باختند.

یادبودی ناچیز برای آنان که هرگز فراموش نخواهند شد.

Contents

| | |
|---|----|
| Introduction | 1 |
| 1.1 Background and Problem Statement..... | 1 |
| 1.1.1 Microplastics as Persistent and Ubiquitous Pollutants | 1 |
| 1.1.2 Ecological and Biogeochemical Risks..... | 2 |
| 1.1.3 Human Health Impacts..... | 3 |
| 1.2 Objectives of the Study..... | 4 |
| 1.3 Research Hypotheses | 5 |
| 1.4 Structure of the Thesis..... | 5 |
| Literature Review | 7 |
| 2.1 Definition | 7 |
| 2.1.1 Classification of Microplastics..... | 8 |
| 2.2 Sources of Atmospheric Microplastics | 11 |
| 2.2.1 Textile Fiber | 11 |
| 2.2.2 Tire Wear Particles | 11 |
| 2.3 Microplastics in Rainfall: Case Studies | 11 |
| 2.4 Knowledge Gaps and Research Needs..... | 13 |
| Materials and Methods | 15 |
| 3.1 Study Area..... | 15 |
| 3.2 Sample Collection..... | 16 |
| 3.3 Sample Preparation | 18 |
| 3.4 Contaminant prevention..... | 19 |
| 3.5 Filter selection..... | 21 |
| 3.6 Filtration Procedure..... | 24 |

| | |
|---|----|
| 3.7 Visual Identification and Classification | 26 |
| 3.7.1 Subsampling and Particle Counting Strategy..... | 27 |
| 3.7.2 Raman instrument settings | 33 |
| 3.7.3 Raman software and spectral libraries | 33 |
| 3.8 Spectral Acquisition and Data Processing | 34 |
| 3.9 Quality Control and Blank Tests | 37 |
| Results | 38 |
| 4.1 Morphological and Chemical Identification of Microplastics | 38 |
| 4.1.2 Raman Spectral Confirmation..... | 40 |
| 4.2 Microplastic Concentration in Rainfall Samples | 41 |
| 4.3 Morphological characteristics | 43 |
| 4.3.1 Color distribution..... | 43 |
| 4.3.2 UV Fluorescence Response | 44 |
| 4.3.3 Polymer composition (Raman confirmed)..... | 46 |
| 4.2.3 Fiber length distribution..... | 48 |
| 4.4 Blank Test Results..... | 50 |
| Discussion..... | 51 |
| 5.1 Microplastic Abundance and Comparison with Previous Studies | 51 |
| 5.2 Statistical Behavior of Microplastic Concentrations | 51 |
| 5.3 Polymer Composition and Potential Sources..... | 52 |
| 5.4 Color Distribution and Environmental Implications..... | 52 |
| 5.5 Fiber length distribution and atmospheric Transport | 53 |
| 5.6 Methodological considerations | 54 |

| | |
|---------------------|----|
| 6. Conclusion..... | 55 |
| 7. References | 56 |

Table of Figures

| | |
|--|----|
| Figure 1. Presence of MPs in different environments. Image Source:[6]..... | 2 |
| Figure 2. The route of microplastics through the food network. Image From [11]..... | 3 |
| Figure 3. Classification of MPs based on the origins. Image from thegreatbubblebarrier.com/what-are-microplastics | 9 |
| Figure 4. The rainfall sampling site is in northern Italy (45.930360° N, 7.539812° E), within the Valle d’Aosta region in the Alpine area..... | 15 |
| Figure 5 . Teledyne ISCO 6712 portable automatic sampler used for rainfall collection: (A) external view of the sampler unit; (B) internal multi-bottle configuration for Adapted from Teledyne ISCO (6712 Portable Sampler User Manual) | 16 |
| Figure 6. Annotated view of the high-altitude monitoring station used for passive rainfall sampling. | 17 |
| Figure 8. Left: samples after the addition of hydrogen peroxide; Right: hydrogen peroxide used in the laboratory..... | 18 |
| Figure 9. Laboratory fume hood (left) and the configuration of the operation table under the fume hood after rinsing (right). | 20 |
| Figure 10. Filters used in the filtration procedure described in Section 3.5, polycarbonate track-etched filter for microplastic analysis (top) and the supporting glass fiber filter placed(bottom)..... | 22 |
| Figure 11. Vacuum filtration and filter handling during rainwater sample processing. (a) Assembly of the vacuum filtration system with aluminum foil covering to minimize airborne contamination. (b) Filtration of hydrogen peroxide–digested samples using polycarbonate membrane filters under a fume hood. (c) Sample processing performed under controlled laboratory conditions using non-plastic protective equipment. (d) Post-filtration handling of the membrane filter with metal tweezers prior to drying and subsequent analysis..... | 25 |
| Figure 12. Hirox Microscope. The digital microscope used in this study. | 26 |
| Figure 13. Schematic representation of the calculation used to determine the analyzed fraction of the polycarbonate filter. The effective filter area was calculated based on the membrane | |

diameter (35 mm, $\approx 960 \text{ mm}^2$). Approximately 12.5% of the total filter surface ($\sim 120 \text{ mm}^2$) was selected for analysis and covered by examining 38–40 non-overlapping microscopic fields of view distributed across the filter surface.....28

Figure 14. Visual comparison of a particle excluded from microplastic identification due to inconsistent morphological features (left) and a suspected microplastic fiber classified based on visual criteria (right).29

Figure 15. Images of multiple fibers, used as a reference for recognizing the microplastic fibers. natural fibers: a: cotton, b: flax, chemp, d: ramie , e: viscose , f: acrylic , g: polyester, h: polyamide eproduced from Cintron *et al.* (2024), *Microplastics*, CC BY 4.0.29

Figure 16. The scheme of Raman principle30

Figure 17. RAMAN Microscope in the lab31

Figure 18. Customized Raman microscope configuration, proper alignment, improved stability of the filter, and facilitated accurate particle tracking during analysis.32

Figure 19. Raman analysis software and spectral libraries used in this study: WiRE 5.7 software interface for Raman data acquisition and processing34

Figure 20. Raman spectra of two representative particles detected on the filtered rainfall sample, shown alongside reference spectra used for polymer identification. Top: an accepted spectrum with quality index 0.82. Bottom: no result confirmation.....36

Figure 21. Representative microscopic images illustrating morphological differences between synthetic microplastic fibers (a–c), cotton fibers (d–f), and organic/natural fibers (g–h) viewed on filter membranes. Synthetic fibers almost show smooth surfaces and uniform diameters, whereas cotton fibers display twisted ribbon-like structures, and organic fibers show irregular, non-uniform morphology.....39

Figure 22. Up: (a) Optical image of white fiber (scale bar=100). (b) Raman spectrum of the analyzed fiber. Peaks are overlaid with the reference library spectrum. Down: (a) optical image of a pink fiber (scale bar = 100). (b): Raman spectrum overlaid with reference spectrum. The values of peaks are equal to the reference spectrum. For both fibers, the match quality is over 90 percent.....40

Figure 23. Microplastic concentration per rainfall sample (particles/L).41

Figure 24. (a) Box plot and (b) histogram showing the distribution of microplastic concentrations (particles/L) across rainfall samples.....42

Figure 25. The number of detected fibers per color category in each sample. The maximum count belongs to white and black, respectively.43

Figure 26. Overall color distribution of microplastic fibers in rainfall samples (n = 189). White (30%) and black (20%) were dominant, followed by transparent (14%) and blue (9%), while the remaining colors each accounted for <10% of total fibers.44

Figure 27. left: SASSO 28 filter under UV light, no fluorescent fibers. Right: SASSO 11. Click to view the full resolution.45

Figure 28. Stepwise identification of fibers detected in 27 rainfall samples. Fluorescence was used as an initial screening step, followed by morphological assessment to classify suspected microplastic (MP) fibers, and final confirmation by Raman spectroscopy. Bars indicate the number of fibers (n) identified at each stage for individual samples.46

Figure 29. Polymer composition across rainfall samples. Raman-confirmed polymer counts (PET, polyester, nylon, acrylic) per sample, showing PET as the dominant type. Click on the image to view in high resolution.47

Figure 30. Overall polymer distribution in rainfall samples. (n = 189).....48

Figure 31. Frequency distribution of microplastic fiber lengths. Histogram showing a right-skewed distribution, with most fibers measuring <1000 μm and a few long-length outliers. ..49

Figure 32. Statistical summary of fiber length distribution. Box plot shows median, interquartile range, and high-length outliers, confirming a positively skewed size distribution.50

Figure 33. Left: Q–Q plot of raw concentration data showing clear deviation from the reference line, indicating non-normal distribution. Right: Q–Q plot of log-transformed concentrations demonstrating improved alignment with the theoretical normal line, confirming log-normal behavior of the dataset.52

Table of Tables

| | |
|---|----|
| Table 1. Morphological classification of microplastic particles, their characteristic features, dominant sources, and key environmental and biological implications. | 10 |
| Table 2. Summary of selected studies on atmospheric microplastics, including study area, sample type, dominant microplastic types, and main findings. | 13 |
| Table 3. Quality assurance and contamination control measures | 20 |
| Table 4. Comparison of commonly used filter materials for microplastic analysis, highlighting their structural characteristics, chemical resistance, spectroscopic suitability, primary advantages, and methodological limitations. | 23 |
| Table 5. The differences between MP particles and Natural or organic particles. These criteria were utilized to determine the Microplastic fibers. | 28 |
| Table 6. Common Raman Parameters. | 33 |
| Table 7. Summary of fluorescent fiber detection, morphological classification, and Raman confirmation in rainfall samples. | 45 |

Introduction

1.1 Background and Problem Statement

The transformative feature and its low price have made plastics one of the primary materials used widely in industry[1]. Nevertheless, overreliance on Plastic materials has increased the production rate. Unfortunately, the production rate is combined with poor waste management, especially in the plastic sector, leading to plastic as a major contributor to the contamination crisis of the current era. Since the beginning of commercial production, the rate of plastic production has steadily increased over the decades.[2]. Although a change in patterns seems essential, the global dependence on synthetic polymers has not changed significantly over the decades. From a statistical perspective, 506 million tons of plastic were produced. This value increased approximately 40 percent over 4 years, from about 259 million tons back then. The massive amount of plastic produced every year inevitably results in significant amounts of plastic debris entering the environment. A large portion of plastic materials ends up in landfills or natural ecosystems. According to reports, around 78 percent of all plastic products are dumped. Seas and oceans have become two major environments in which plastic is disposed[3]. The volume of plastic entering the seas and oceans is unbelievable. This value is about 4.8 to 12.7 million metric tons that are released to the marine environment [3]. These numbers are a warning about the seriousness of plastic contamination.

1.1.1 Microplastics as Persistent and Ubiquitous Pollutants

Among other environmental pollutants, microplastics are considered the most serious and widespread [4]. The key difference between microplastics and other pollutants is several factors. The most important one is that they are durable in the environment due to their resistance to natural degradation. In addition, microplastics are widely distributed across the Earth. Besides, scientific evidence shows that microplastics can interfere with biological systems [5]. Microplastics are called ubiquitous because their presence has been traced in every type of environment. Once it was believed they were limited to the marine environment, but their presence is now widely recorded in other environments, such as freshwater, soils, and even runoff [4] (Figure 1). They are found even in most pristine environments, such as the deepest

parts of the oceans and seas. Compared to surface water, MP concentrations are higher in deep regions. Therefore, seafloor and deep-sea waters are significant sinks of MP[4]. A similar pattern occurs in terrestrial soils. Resources such as agricultural runoff, wastewater treatment, and atmospheric deposition scatter and contribute to the accumulation of MP on land[5].

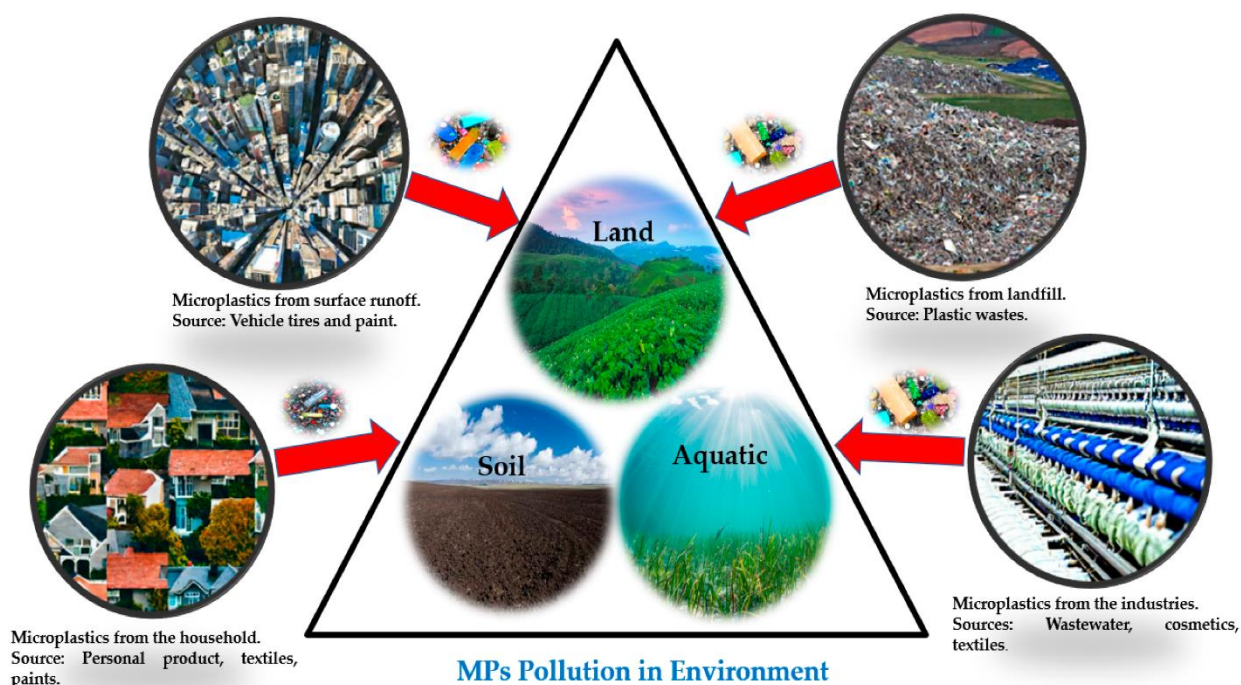


Figure 1. Presence of MPs in different environments. Image Source:[6]

1.1.2 Ecological and Biogeochemical Risks

Due to their chemical composition, MP particles undergo chemical reactions with other elements, such as carbon and nitrogen[7]. That is why even biogeochemical processes may be manipulated by MP. Consequently, in the terrain, soil composition and configuration can be altered. MP can have an effect even in microscopic scale. It can modify vital activities of enzymes in marine and terrestrial systems[8].

From a broader perspective, the entire process of the plastic lifecycle, starting from extraction until disposal, produces greenhouse gas emissions, which are directly linked to climate change. In this way, the negative impacts of climate change can even increase the toxicity and

distribution rate of microplastics[9]. The MP is harmful for the total living organism, from plankton to apex predators. Its negative effects go beyond physical damage. Multiple health impairments, such as feeding efficiency and malnutrition, are other effects of the MP in living organisms, because the MP surface can increase the rate of toxic absorption within the body[10]. Moreover, these negatives may even be exacerbated by the chemical additives adhering to the MP itself. All these elements, combined, set the stage for the pollution of food webs[9].

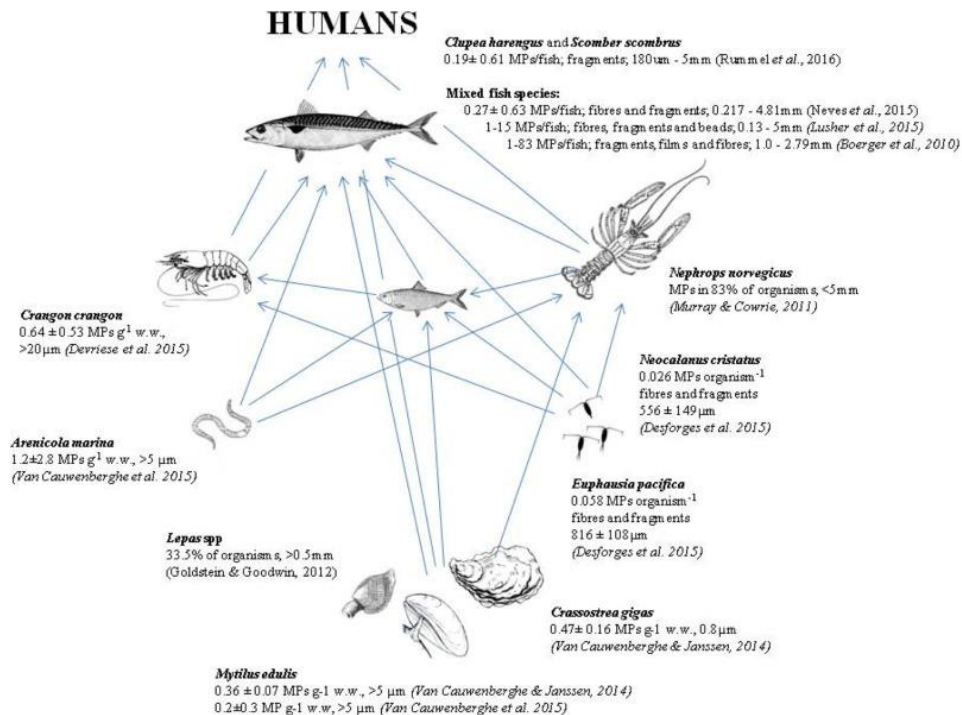


Figure 2. The route of microplastics through the food network. Image From [11]

1.1.3 Human Health Impacts

There is still no clear answer to whether human exposure to MP has long-term effects on health. The topic is still under study. However, microplastic particles can enter the human body through multiple pathways (Figure 2)[12]. Already-contaminated food can potentially allow MP to pass inside the body. The ambient air in which MP is suspended could provide the same route of exposure via inhalation[13]. So far, evidence shows that health disorders such as metabolic disruption and immune system illnesses are likely associated with microplastic exposure [14].

1.2 Objectives of the Study

The main objective of this study is to assess the efficiency of the common method and refine the methodological approach, and optimize the workflow related to preparing and analyzing rainfall samples by Raman spectroscopy. To determine the concentration of MP fibers in rainfall samples from Valle d'Aosta. Finally, investigation of the morphological and physical characteristics of MP fibers, including color and size, are the other purpose of this study.

1.3 Research Hypotheses

Based on existing literature on atmospheric microplastics and their deposition through precipitation, this study is guided by the following hypotheses:

H1. The presence of microplastic particles has been proven in previous studies across a wide range of environments. atmospheric factors such as wind contribute to scattering the microplastics,[15] which cause their presence in environments like urban, rural, and even remote regions [16]. Hence, it is assumed that rainfall samples collected at the Sasso station contain microplastics.

H2: Fibrous microplastics represent the dominant morphological type in rainfall samples [16] The most dominant type of microplastic in rainfall samples is Fibrous. According to previous studies, the abundance of fibrous MPs is higher than that of other types, such as films and fragments. Low density and aerodynamic features facilitate the distribution of them through the environment [17]. Speaking of their origin, textile abrasion and household activities are considered the top resources[18]. Consequently, in this study, we hypothesize that fibrous microplastics will constitute the majority of MPs in the rainfall samples.

1.4 Structure of the Thesis

This thesis is written in six chapters. In the first chapter, we provided a general overview of plastic pollution and its problematic nature. In addition, the negative environmental impacts of microplastics are explained. At the end of this chapter objectives and hypotheses of the study are described.

Chapter 2 is a recap of the current literature regarding microplastics. It aims to present a definition of microplastics that considers size, chemical characteristics, and morphology. Furthermore, it offers a comprehensive overview of the current literature and the latest findings on microplastics.

Chapter 3 is about the materials and methods used in this study. After introducing the study location and the sampling collection, it fully explains the materials required to perform the relevant analysis. Also, the methodology followed in the research.

Chapter 4 presents the study's results, organized into 5 sections. Multiple visual analyses are presented in the first section, followed by results reporting the concentration of microplastic

fibers. Other chapters explain the morphological and physical characteristics of the confirmed MP fibers, including color and length distribution.

In chapter 5, the focus is on the interpretation of the results. The discussion covers microplastic abundance and the statistical behavior inferred from the concentration results. Similarly, multiple hypotheses are proposed regarding potential sources of microplastics based on polymer composition and fiber-length distribution. At the end of this chapter, several methodological considerations are suggested too.

Literature Review

2.1 Definition

The exact definition of microplastic has changed several times. Effectively, once a loose descriptive label is now turned into a formalized regulatory metric [19]. However, there is still no general agreement upon its true definition across scientific disciplines. Historically, early marine litter surveys were the first to detect tiny plastic particles in the Atlantic Ocean. But these were not counted as a potential threat back then; they were considered more like curiosities. In the early 21st century, the focus was altered, and those micro fractions were considered a distinct group of pollutants [20].

It was after a workshop hosted by NOAA in 2008 that the definition of microplastic was assigned to any plastic particles whose largest dimension is smaller than 5mm. This definition is now adopted by many regulatory and scientific bodies, such as the United Nations Environment Program (UNEP), the European Chemicals Agency (ECHA), and GESAMP, providing a necessary baseline for global monitoring efforts [21], [22].

Considering 5mm, the upper limit is not a random option. In fact, this value is defined based on ecological considerations and the need to keep coherence and practicality in existing approaches.

Ecological Interaction: The 5 mm threshold corresponds to the size of prey items for a wide range of aquatic organisms, such as small fish, crustaceans, and seabirds. Particles of this size are small enough to be ingested but large enough to cause physical blockage of the gastrointestinal tract, a distinct mechanism of harm compared to the entanglement risks posed by larger macroplastics[23].

Regulatory Pragmatism: to be easily visualized is another significant criterion for some agencies, such as NOAA. In this regard, 5mm is an appropriate size for policy and public outreach. This value is frequently expressed “about the size of the pencil eraser [24].

Although the 5mm threshold is commonly used, still criticism remains toward it. Some researchers contend that this cutoff is not sufficient in terms of biological justification, meaning no abrupt shift occurs in toxicity or environmental impact. Nevertheless, the 5mm threshold is still a standard value to reach a unified and harmonious[25].

2.1.1 Classification of Microplastics

In addition to their size, microplastic particles possess specific physicochemical properties that distinguish them from other environmental materials. microplastics need to be synthetic in origin [34]. To make a plastic material, generally petroleum-based polymers such as polyethylene, polypropylene, and polystyrene, as well as bio-based synthetic polymers, are used[35]. In contrast, naturally occurring polymers, such as unmodified cellulose, are typically excluded from this definition [27]. On the other hand, semi-synthetic materials such as rayon and cellophane are often included in environmental studies due to their anthropogenic origin, widespread use, and persistence in the environment [36].

2.1.1.1 Classification: Primary vs. Secondary Microplastics

Primary Microplastics: Intentionally Microscopic: Many microplastics are not produced through weathering or fragmentation; they are intentionally manufactured at very small sizes. Their applications are designed for specific industrial, commercial, and medical purposes. These particles enter the environment at their original size, often through wastewater discharge or industrial spills.

Secondary Microplastics: The Unintentional Majority .Unlike primary microplastics, secondary microplastics result from the fragmentation or weathering of larger plastics. In fact, a larger plastic object gets smaller through mechanical or chemical processes in nature. A huge part of the MP found in nature belongs to this sort. Their presence is deeply rooted in discarded bottles, bags, and construction debris that are often improperly disposed of[26].

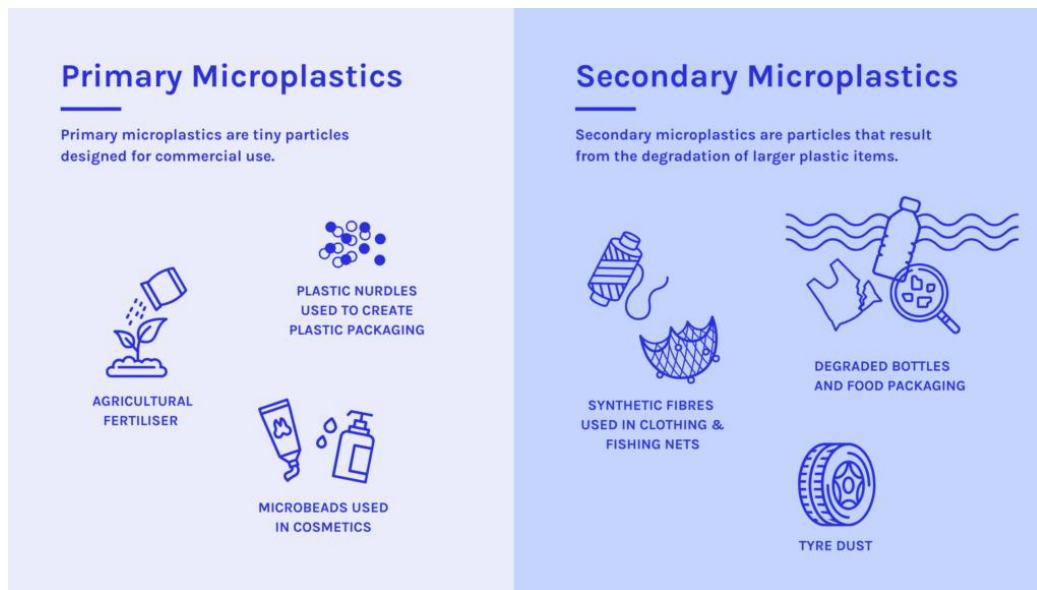


Figure 3. Classification of MPs based on the origins. Image thegreatbubblebarrier.com/what-are-microplastics

2.1.2 Shape categories: Morphology as a fingerprint

The shape, or morphology, of a microplastic particle is as critical as its size [27]. Morphology often provides the "fingerprint" of the particle's origin (source location) and reveals its interactions with biota (e.g., ingestion dynamics, settling velocity, gut retention time). Current classification schemes typically recognize five main categories of microplastic shapes: **Fibers, Fragments, Films, Foams, and Pellets/Beads** [28].

Table 1. Morphological classification of microplastic particles, their characteristic features, dominant sources, and key environmental and biological implications.

| Morphology | Description | Main Sources | Key Environmental / Biological Notes | References |
|-------------------|--|---|--|---|
| Fibers | Elongated, thread-like particles | Synthetic textiles, fishing gear, cigarette filters | Most common form in atmospheric and deep-sea samples; easily transported; often retained longer in digestive systems | Dris et al., 2016; Hidalgo-Ruz et al., 2012 |
| Fragments | Irregular, rigid particles with broken edges | Breakdown of rigid plastic items | Typical secondary microplastics; sharp edges may cause physical damage upon ingestion | Andrady, 2011; Cole et al., 2011 |
| Films | Thin, flexible, sheet-like particles | Plastic bags, mulch films, packaging | Easily transported by wind; float initially in water; affect soil structure in agricultural areas | GESAMP, 2015; Zhang et al., 2020 |
| Foams | Porous, lightweight particles | Expanded polystyrene products | Highly buoyant; strong capacity to adsorb organic pollutants | Andrady, 2011; GESAMP, 2015 |
| Pellets / Beads | Spherical or cylindrical particles | Industrial pellets, cosmetic microbeads | Indicate primary pollution sources; easily mistaken for food by wildlife | Cole et al., 2011; Hidalgo-Ruz et al., 2012 |

2.2 Sources of Atmospheric Microplastics

Different point sources linked to anthropogenic activities collectively contribute to the release of microplastics into the atmosphere. In this process, not only do industrial activities play a key role, but many individuals' everyday activities are also involved. Regarding dominant sources, textile fibers, tire wear particles, and urban and industrial dust continuously generate airborne microplastic pollution.

2.2.1 Textile Fiber

Studies show that the primary source of atmospheric microplastics (MP) is synthetic textile fibers. Several pathways have been identified as mechanisms for generating this type of MP. Some seemingly simple actions are responsible for it. For example, microplastic fibers can be released when wearing clothes. Similarly, household activities, including laundry, can introduce MP into the ambient air. To clarify, routine tasks like washing clothes that involve mechanical abrasion may produce thousands of microplastic fibers into indoor and outdoor environments. This amount can be dispersed by ventilation systems and wastewater treatment processes. Textile fibers can be easily suspended in air because their elongated shape increases their surface area-to-volume ratio. For the same reasons, they can be easily transported by air and reach remote regions far from their original source.

2.2.2 Tire Wear Particles

Another source of MP particles is tire wear particles. Tire wear consists of a complex composition that includes synthetic rubber polymers. Although its contribution to MP contamination is often underestimated, researchers rank these polymers among the main microplastic emitters. MP particle generation occurs through friction between tires and road surfaces. This level of MP release is particularly high in urban areas due to their high traffic volume.

2.3 Microplastics in Rainfall: Case Studies

Recent studies have established a direct correlation between atmospheric microplastic deposition and proximity to human activities. These quantities are shown in the study of Wright et al. (2020). His results reported 712 fibres/m²/day in the urban area of London. Similar results occur in other studies. For instance, in Mutshekwa et al. (2025) investigation,

the urban peak was around 355.6 fibers/m²/day in South Africa. However, a growing body of literature has started to emphasize the development of this topic in pristine regions, recognizing the intensity of MP transformation in the environment. Mutshekwa et al. (2025) estimated that tons of MP are deposited in forests, despite being far from urban areas.

Recent literature agrees that rainfall is an effective means of scattering atmospheric MP over land. But it is still unclear how intense it is. To accomplish a valid estimation, (Wright et al., 2020) in London and (Mutshekwa et al., 2025) in South Africa (Mutshekwa et al., 2025) have done research. Passive sample collection and an uncovered container were two considerations in their study. Because that was prone to mixing up the washed and dried microplastic particles. To address this issue, Villafañe & Ronda (2023) in Argentina used an active collector. Nevertheless, this kind of collector is rarely used in other literature, and further studies are required. All in all, the efficiency of rainfall to capture MP remains under question.

Table 2. Summary of selected studies on atmospheric microplastics, including study area, sample type, dominant microplastic types, and main findings.

| Author and Year | Location | Sampling Method & Duration | Findings |
|-------------------------|--|---|--|
| Mutshekwa et al., 2025 | Thulamela Local Municipality, South Africa (Urban, rural, and forest subtropical environments) | Passive samplers (bulk deposition) over 6 weeks | Forest MP deposition showed a strong positive correlation with rainfall, indicating rain |
| Villafañe & Ronda, 2023 | Bahia Blanca, Argentina (Urban/Coastal) | Active wet-only collector (open only during rain events) over 10 months | First assessment of MP pollution in rain in Argentina. |
| Wright et al., 2020 | Central London, UK (Urban) | Atmospheric deposition (bulk) sampled every 3-4 days | High deposition rates in a major urban center |
| Dris et al., 2016 | Greater Paris, France (Urban and Sub-urban) | Atmospheric fallout (bulk deposition) | Higher levels of MPs are found in urban sites due to intensified anthropogenic activities and higher population density. |
| Klein & Fischer, 2019 | Hamburg Metropolitan area, Germany (Urban and Rural/Forest) | Bulk precipitation samplers collected twice-weekly over 12 weeks (winter) | Unexpectedly higher concentrations were found in rural/forest sites |

2.4 Knowledge Gaps and Research Needs

One major gap is related to the sample collection type. While many studies have employed passive collection, a limited number of studies have used an active collection sampler. Therefore, a passive sampler may introduce errors to the results. The reason is that microparticles in the container may be a mix of airborne MP and MP originating from other environments, such as land.

Although many studies have used digital scanning, the confirmation of MP is not guaranteed by this technique. Therefore, to enhance confidence, chemical confirmation by Raman microscopy is required. On the other hand, Raman microscopy has its own weaknesses, such as fluorescence interference and low-quality signals. As a result, a combination of the mentioned techniques and associated methodology is not fully discussed in similar studies.

Additionally, Many case studies focus on large urban areas or a small number of remote locations, where the anthropogenic activities are minimal. This limits the ability to deeply understand any effect of local versus long-range atmospheric sources and to understand how meteorological factors, such as rainfall intensity and wind patterns, influence microplastic deposition[29], [30].

Materials and Methods

3.1 Study Area

Alps at geographic coordinates 45.930360° N, 7.539812° E. The sampling site is located at an elevation of approximately 2415 m above sea level. (Figure 4)

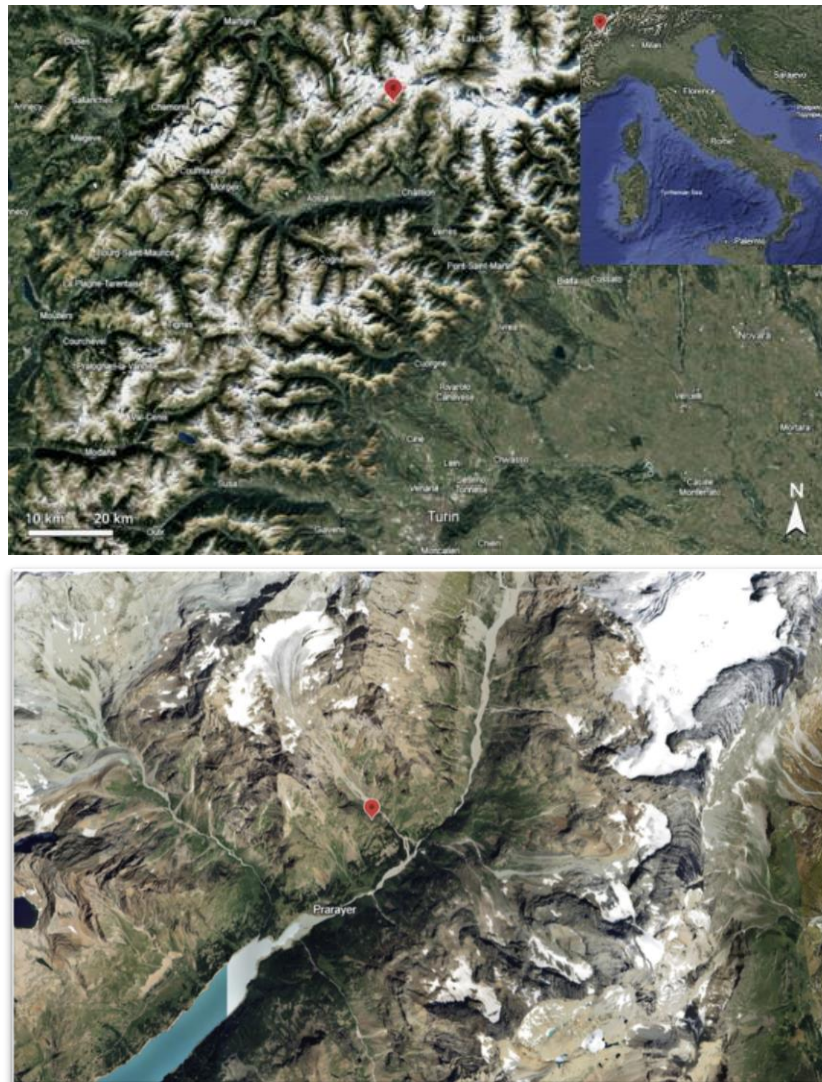


Figure 4. The rainfall sampling site is in northern Italy (45.930360° N, 7.539812° E), within the Valle d’Aosta region in the Alpine area.

The area is characterized by steep terrain and poor accessibility, with access primarily provided through mountain hiking trails. The surrounding landscape is predominantly alpine, with sparse vegetation cover. In terms of anthropogenic activities, human-built infrastructure is

rare. There is no city close to the site. In addition, industrial activities are far from the location, making the area representative of a remote mountainous environment.

Since this study site is in high elevation and it is very isolated, the study location is subjected to strong atmospheric processes, including long-range air mass transport and orographic precipitation. Such conditions make high-altitude alpine sites perfect for investigating atmospheric deposition processes, including the transport and deposition of microplastics via rainfall. The absence of local emission sources allows the influence of regional and long-range atmospheric inputs to be assessed with reduced interference from direct anthropogenic activities.

3.2 Sample Collection

27 Rainwater samples were collected, from early June to late July 2025, using a active precipitation sampling system (Teledyne ISCO 6712 Portable Sampler) (**Figure 5**) installed in an open area of the monitoring station [31]. The sampler was placed at an elevated height above ground level to allow direct collection of precipitation and to limit secondary contamination from soil resuspension or nearby surfaces. The details of the collection system are shown in **Figure 6**.

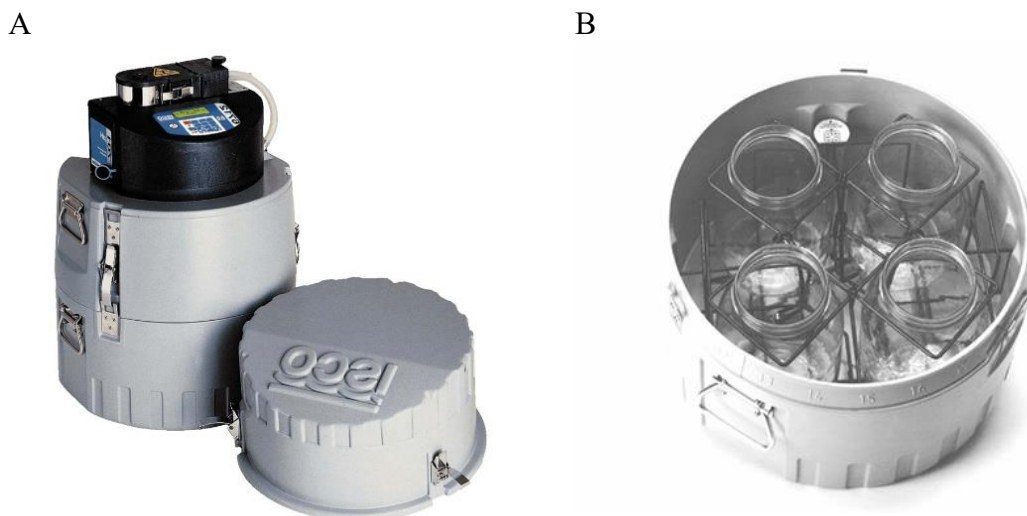


Figure 5 . Teledyne ISCO 6712 portable automatic sampler used for rainfall collection: (A) external view of the sampler unit; (B) internal multi-bottle configuration for
Adapted from Teledyne ISCO (6712 Portable Sampler User Manual)

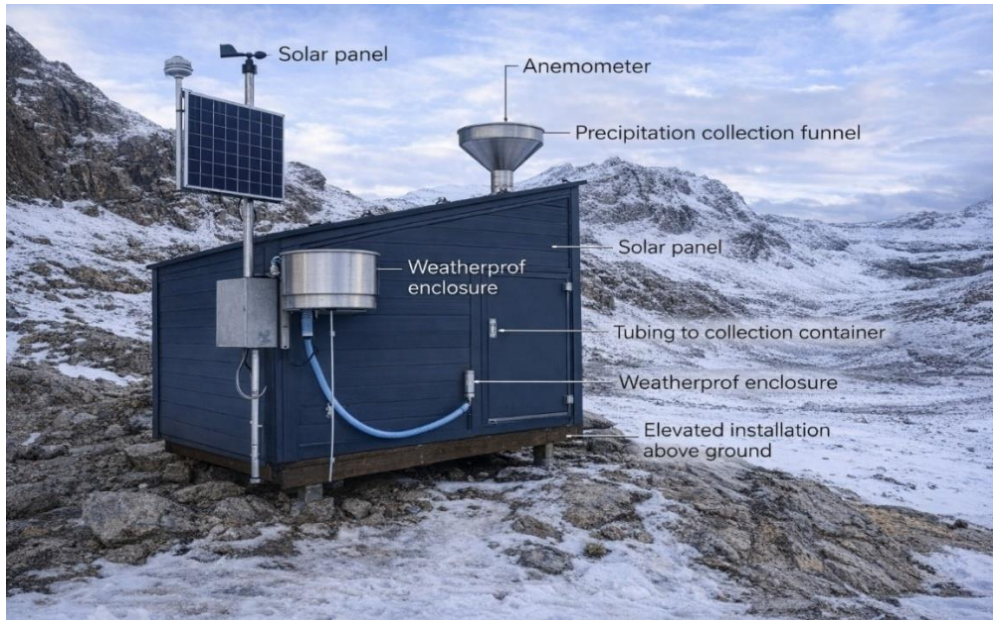


Figure 6. Annotated view of the high-altitude monitoring station used for passive rainfall sampling.

The sampling system consisted of a precipitation collector connected to a sealed container housed within a protective enclosure. The system operated with no mechanical pumping. It relies exclusively on natural rainfall deposition. During precipitation events, rainwater was directly poured into the sampling container. Strict contamination control measures were applied throughout the sampling and handling procedures. All sampling components in contact with rainwater were made of non-plastic materials such as glass and metal whenever possible. Containers and tools were thoroughly cleaned before use. Direct contact with plastic materials was avoided during sample collection, transport, and storage to decrease the risk of external microplastic contamination.

3.3 Sample Preparation

All rainfall samples were stored in 300 mL glass jars and refrigerated until laboratory analysis [32]. Before the filtration process, the samples required preparation steps aimed at removing soluble and non-plastic materials commonly present in rainfall, such as organic matter and mineral residues [43]. After transferring the samples to the laboratory, they were allowed to reach room temperature before further processing. As shown in Figure 8, to remove organic material from the rainfall samples, hydrogen peroxide (60%) was used as a digestion agent [50]. This chemical treatment facilitated the breakdown of organic matter, thereby improving the visibility and detection of microplastic particles during subsequent analysis [51]. For the first six samples, a hydrogen peroxide-to-rainwater ratio of 1:5 was applied. For the remaining samples, this ratio was adjusted to 1:1 to improve digestion efficiency. After measuring the exact volume of each sample, the predetermined amount of hydrogen peroxide was added, and the mixtures were thoroughly agitated in glass containers. [33]The treated samples were then left to react for five days under laboratory conditions before the beginning of the filtration process [34].

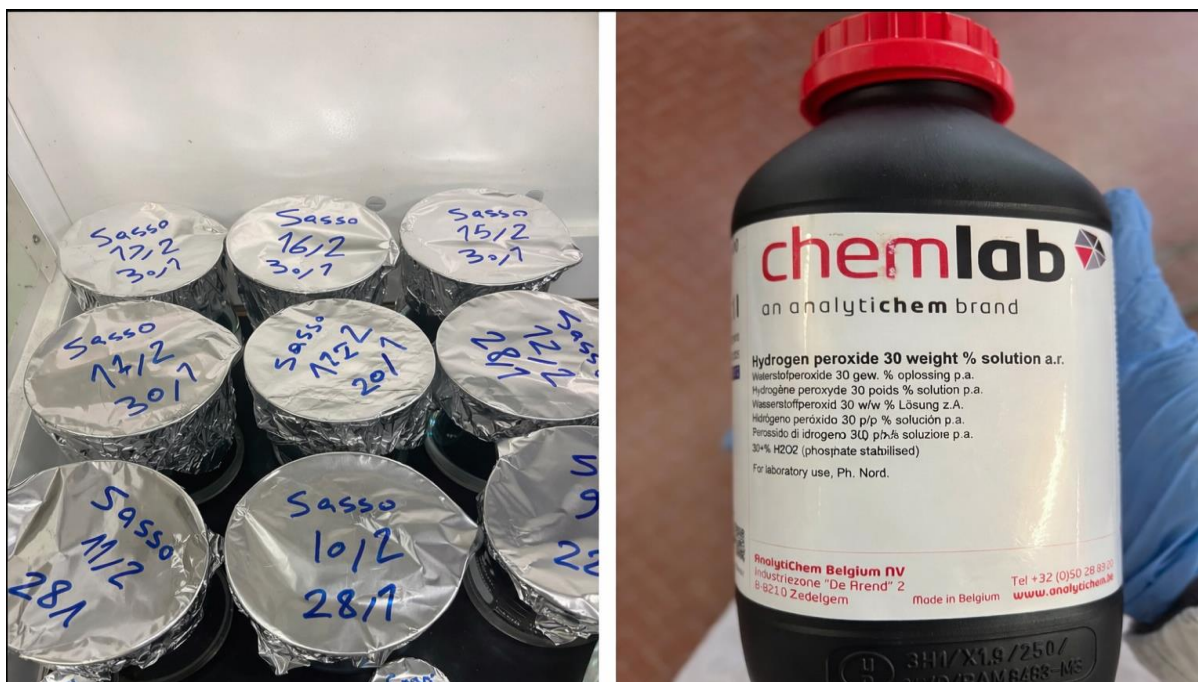


Figure 7. Left: samples after the addition of hydrogen peroxide; Right: hydrogen peroxide used in the laboratory.

3.4 Contaminant prevention

To avoid any possible contamination, strict protocols were set and followed. Glass jars, used to keep the rainfall sample, were completely rinsed and washed. Then they were sealed with stainless lids to keep them away from plastic materials during storage. All equipment and tools that came into contact with the samples were thoroughly cleaned prior to use. Washing solutions, including ethanol, were filtered two times to remove potential background contaminants. Similarly, Milli-Q water was filtered twice before being used for cleaning procedures. Tweezers, beakers, and other glassware were carefully washed using filtered ethanol followed by filtered Milli-Q water. All sample preparation and filtration procedures were conducted under a laboratory fume hood to reduce exposure to airborne microplastics. During laboratory work, operators wore non-plastic gloves and cotton laboratory coats to minimize any possible contamination from synthetic fibers [35]. In addition, the working surface inside the fume hood was fully covered with aluminum foil, preventing direct contact between laboratory tools and any plastic materials. Chemical digestion of organic matter was performed using hydrogen peroxide (60%), [36] applied under controlled conditions to enhance the diagnosing of microplastic particles without introducing plastic-based reagents. All digestion steps were carried out in glass containers, and samples were left to react under laboratory conditions prior to filtration. These quality assurance measures were continuously applied during the experimental procedure to guarantee data reliability and to minimize contamination risks associated with microplastic analysis. Please see **Figure 9**, in which the configuration of the laboratory works is described briefly.

Table 3. Quality assurance and contamination control measures

| Category | Measure Applied |
|---------------------------|---|
| Sample storage | Glass containers with stainless-steel lids; refrigerated storage |
| Reagents & tools | Double filtration of ethanol and Milli-Q water; cleaning of all glassware |
| Laboratory environment | Sample preparation and filtration performed under a fume hood |
| Operator precautions | Use of non-plastic gloves and cotton laboratory coats |
| Work surface | Aluminum foil covering to avoid plastic contact |
| Sample preparation | Digestion in glass containers using hydrogen peroxide (60%) |
| Filter handling | Metal tweezers used; filters covered with aluminum foil after filtration |
| Microscopy & spectroscopy | Visual pre-screening; exclusion of spectra affected by fluorescence or thermal damage |



Figure 8. Laboratory fume hood (left) and the configuration of the operation table under the fume hood after rinsing (right).

3.5 Filter selection

Before filtration, several filter types and pore sizes were evaluated. Selecting an appropriate filter required balancing particle retention, filtration efficiency, and the risk of filter clogging, particularly due to the presence of residual organic matter in the samples. In detail, an appropriate filter for our study must be without any distortion on its surface. This contributes to gathering all similar-sized particles within one focus. In terms of hole size, it has to be smaller than the minimum size of the particles that are under investigation.[37] The main filter types considered are summarized in **Table 3**. Based on these initial considerations, glass fiber and polycarbonate (PC) filters were selected as the primary candidates for the filtration process. **(Figure 10)**

Preliminary tests were conducted using an external water sample to evaluate the performance of each filter type under laboratory conditions. One of the main challenges encountered during these tests was filter distortion after filtration. It was observed that after water filtration and the subsequent drying process, the filter surfaces lost their smooth and flat structure, which made microscopic analysis more difficult. This issue occurred with both glass fiber and polycarbonate filters. To address this problem, an additional filter layer was placed beneath the glass fiber filter. This second supporting layer improved the mechanical stability of the top glass fiber filter during filtration and drying, reducing deformation caused by water flow. Despite this improvement, another limitation was identified during spectroscopic analysis. In several cases, glass fiber filters showed poor tolerance to the Raman laser, and localized burning of the filter material was observed during Raman measurements. Considering these limitations, particularly the deformation after drying and the sensitivity to Raman laser exposure, polycarbonate (PC) filters were ultimately selected as the most suitable option for this study. The flat and uniform surface of PC filters provided better stability during microscopic observation and improved compatibility with Raman analysis. These initiatives make them more suitable for reliable microplastic identification. The filtration procedure applied in this study is described in detail in the following section.



Figure 9. Filters used in the filtration procedure described in Section 3.5, polycarbonate track-etched filter for microplastic analysis (top) and the supporting glass fiber filter placed(bottom).

Table 4. Comparison of commonly used filter materials for microplastic analysis, highlighting their structural characteristics, chemical resistance, spectroscopic suitability, primary advantages, and methodological limitations.

| Filter | Structure | Chemical Resistance | Direct Spectroscopic Suitability | Pros | Cons |
|--------------------------|---------------------------|---------------------|-----------------------------------|---|---|
| Glass Fiber (GF) | Depth / Fibrous | Excellent | Poor (high background, non-flat) | High flow rate, low clogging, chemically inert | Requires particle transfer or specialized reflection mode |
| Polycarbonate (PC) | Surface / Membrane | Moderate to Good | Excellent (when flat or coated) | Flat, uniform surface; ideal for automated imaging/counting | Prone to clogging; requires metal coating for Raman/IR reflection |
| Cellulose Esters (CA/CN) | Surface / Membrane | Poor / Low | Poor (organic interference) | Low cost, readily available | Degraded by strong oxidizers; high organic background |
| Silicon (Si) Wafer | Substrate / Non-polymeric | Excellent | Excellent (FTIR/Raman compatible) | Allows FTIR transmission below 1300 cm^{-1} | Specialized, expensive, sensitive to mechanical damage |

3.6 Filtration Procedure

To filter the rainfall samples, the polycarbonate (PC), with a pore size of 45 μ m was used, as shown in Figure 10. In practice, two obstacles may appear during filtration, namely rapid clogging and microplastic retention on the filter. These are common challenges in the filtration of liquids, especially those containing residual organic matter [38]. Rainwater samples treated with hydrogen peroxide were filtered after a 5-day digestion period. Filtration was carried out using a vacuum filtration system, which is widely applied in microplastic studies due to its efficiency and ability to process relatively large sample volumes in a controlled manner. Prior to filtration, all components of the filtration setup were assembled in advance to minimize sample handling and reduce the risk of contamination. When filtration ended, we grabbed the filter from the filtration unit. This was done with great care to reduce the risk of damage to the filter. After removal, the filter was put in a petri dish. Then they were tightly covered with aluminum foil. The filtered samples were then left to dry under controlled laboratory conditions until further microscopic and spectroscopic analysis. This handling and storage procedure follows commonly recommended practices for microplastic sample preparation and helps preserve particle integrity prior to identification and characterization[39]. **Figure 10** represents the steps of the filtration procedure.

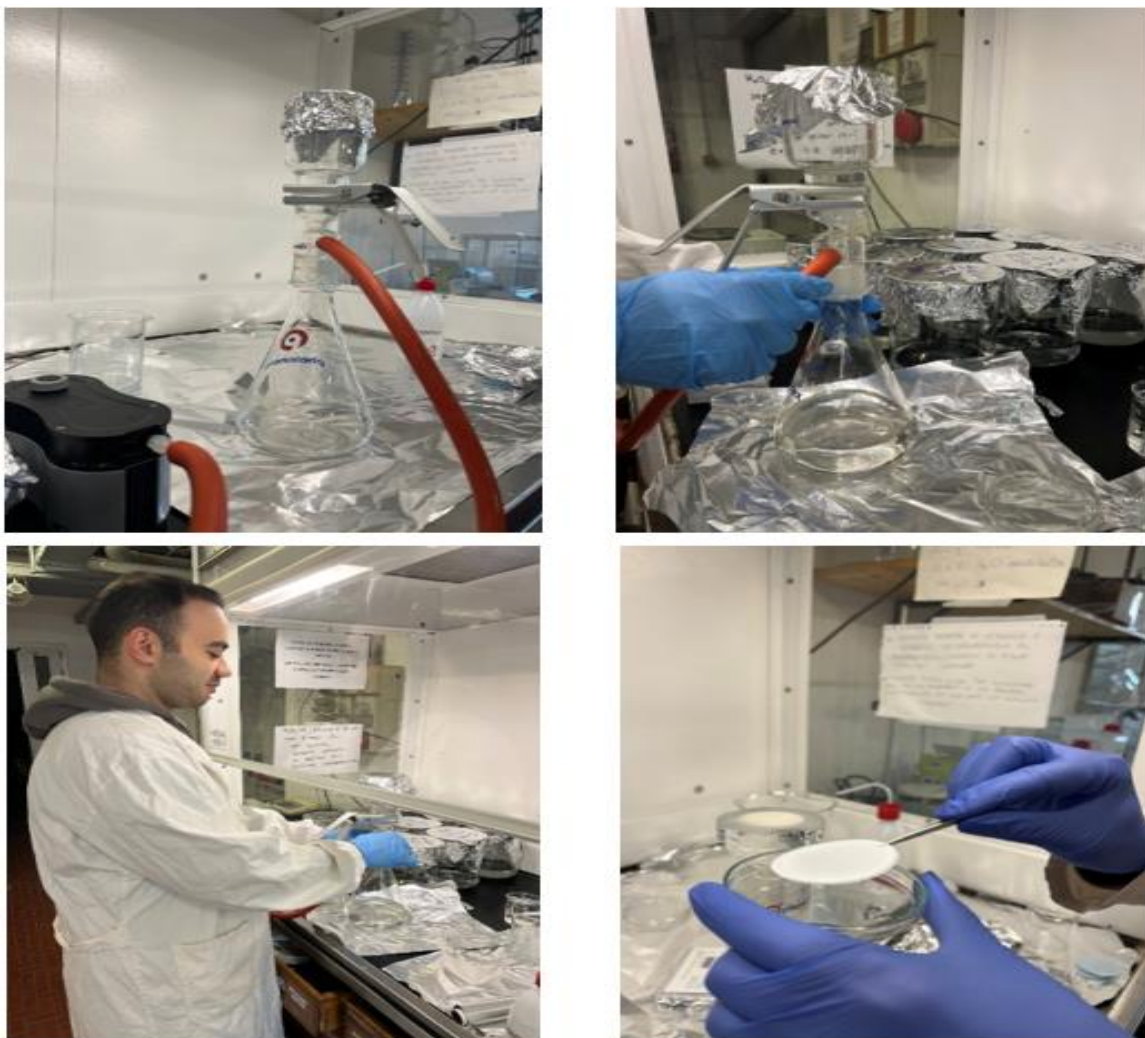


Figure 10. Vacuum filtration and filter handling during rainwater sample processing. (a) Assembly of the vacuum filtration system with aluminum foil covering to minimize airborne contamination. (b) Filtration of hydrogen peroxide–digested samples using polycarbonate membrane filters under a fume hood. (c) Sample processing performed under controlled laboratory conditions using non-plastic protective equipment. (d) Post-filtration handling of the membrane filter with metal tweezers prior to drying and subsequent analysis.

3.7 Visual Identification and Classification

The filtered samples were examined using a digital microscope (Hirox, Japan; model KH-series), Figure 12. As the microscope had been recently installed in the laboratory, an initial period was required to become familiar with the appropriate settings and configurations. During this phase, different imaging options, magnification ranges, and lighting conditions were tested to obtain optimal image quality for microplastic identification.



Figure 11. Hirox Microscope. The digital microscope used in this study.

To obtain a general view of the entire filter surface, the tiling function of the microscope was used. This feature automatically stitched multiple high-resolution images, producing a complete image of the filter while preserving fine details. The quality of the resulting images depended on both magnification and illumination settings. Initially, a magnification of 50 \times was applied to generate a general map of the filter surface. Subsequently, higher magnifications of 140 \times , 600 \times , and 800 \times were used for detailed observation, measurement, and morphological analysis of individual suspected particles. Higher magnification proved particularly useful for examining surface texture, edge characteristics, and internal structure, which are important criteria for distinguishing microplastics from natural materials.

An additional feature of the microscope was the coordinate mapping tool. This function enabled the precise determination of the x–y coordinates of selected particles on the filter surface. By recording these coordinates, specific particles could be reliably relocated for further analysis using Raman spectroscopy, ensuring consistency between visual identification and chemical confirmation.

To measure the particles' length and width, the microscope's default tools were used. By this feature, we could measure the fiber size instantly, significantly reducing analysis time. In contrast, many similar studies have relied on third-party software, such as ImageJ, for particle size analysis.

3.7.1 Subsampling and Particle Counting Strategy

During the analysis of the initial filters, the number of fiber particles observed on the filter surface was too high. Therefore, complete counting and characterization within a reasonable time frame was not feasible. To overcome this challenge, the subsampling method was adopted, following strategies commonly reported in the literature for microplastic analysis [40]. In some cases, depending on the total number of fibers observed on each filter, different subsampling areas were considered. In 7 filters, more than 100 fibers (including natural, organic, and plastic fibers) were identified. In these cases, analyzing half of the filter would have been extremely time-consuming; therefore, only 12.5% of the total filter surface was examined. For filters with fewer detected fibers, 50% of the filter area was analyzed to improve the representativeness of the results. Previous studies have demonstrated that analyzing 12.5% of the filter area can provide a representative estimation of microplastic abundance in environmental samples while significantly reducing analysis time [55].

The selected filter area was systematically divided into multiple fields of view (FOVs) to ensure consistent coverage. For the 12.5% subsampled filters, a total of 40 fields of view were analyzed (Figure 13). All suspected microplastic particles observed within each field of view were documented, measured, and classified based on their morphological characteristics.

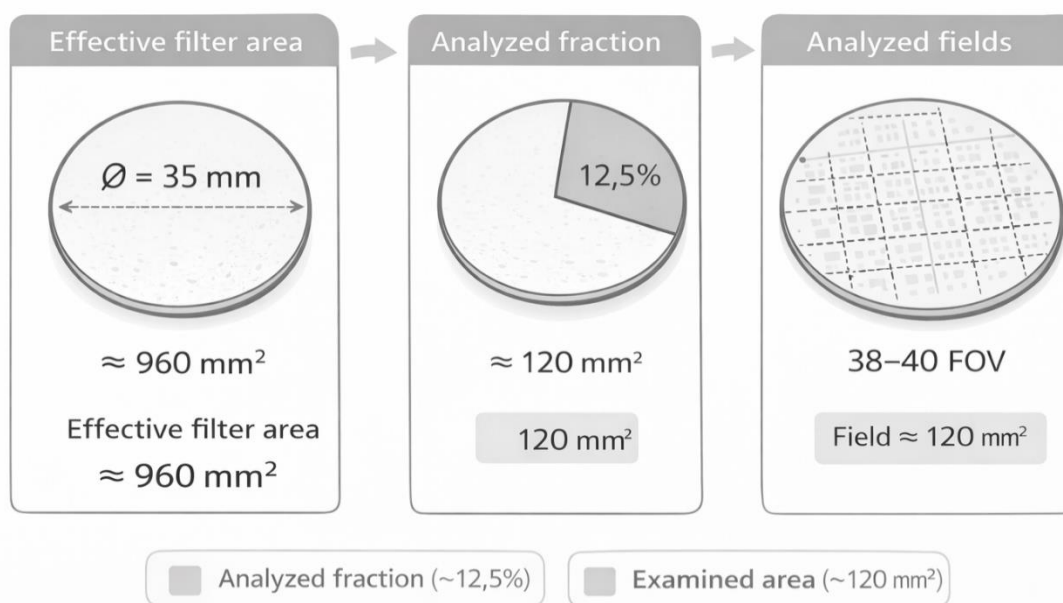


Figure 12. Schematic representation of the calculation used to determine the analyzed fraction of the polycarbonate filter. The effective filter area was calculated based on the membrane diameter (35 mm, $\approx 960 \text{ mm}^2$). Approximately 12.5% of the total filter surface ($\sim 120 \text{ mm}^2$) was selected for analysis and covered by examining 38–40 non-overlapping microscopic fields of view distributed across the filter surface.

Table 5. The differences between MP particles and Natural or organic particles. These criteria were utilized to determine the Microplastic fibers.

| Characteristic | Microplastic Particles | Natural / Organic Particles | References |
|------------------------|---|--|------------|
| Surface texture | Smooth, glossy, or uniform | Rough, matte, or irregular | [39] |
| Edge appearance | Sharp, clean-cut, or angular | Tapered, frayed, or uneven | [39] |
| Color | Homogeneous and uniform | Natural and heterogeneous | [21] |
| Thickness | Relatively constant | Variable | [39] |
| Internal structure | No visible cells, fibers, or membranes | Cellular or fibrous structures visible | [39] |
| Texture/porosity | Solid, non-porous | Fibrous or porous | [41] |
| Manufacturing features | Molding lines or shear marks may be present | Absent | [41] |

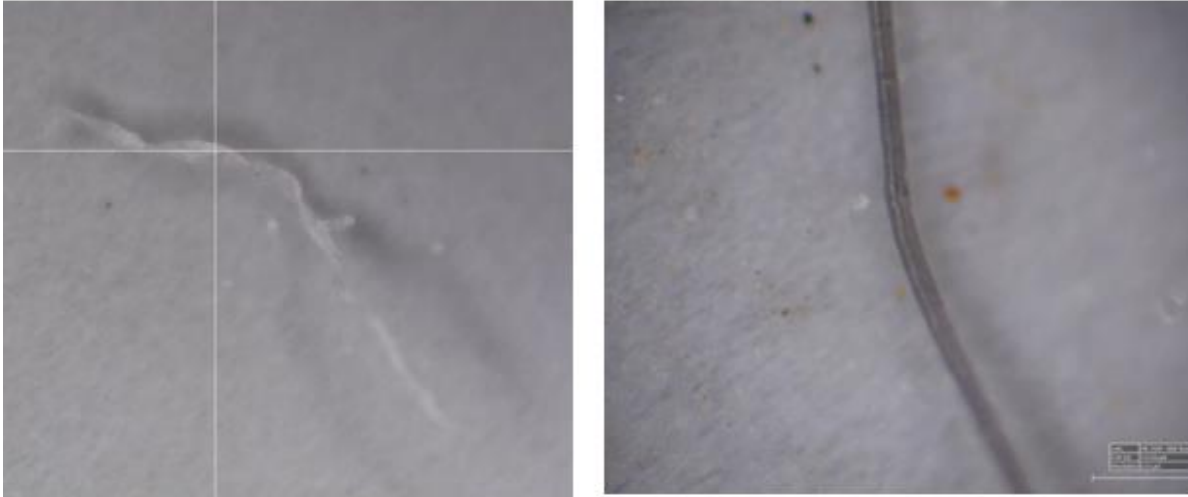


Figure 13. Visual comparison of a particle excluded from microplastic identification due to inconsistent morphological features (left) and a suspected microplastic fiber classified based on visual criteria (right).

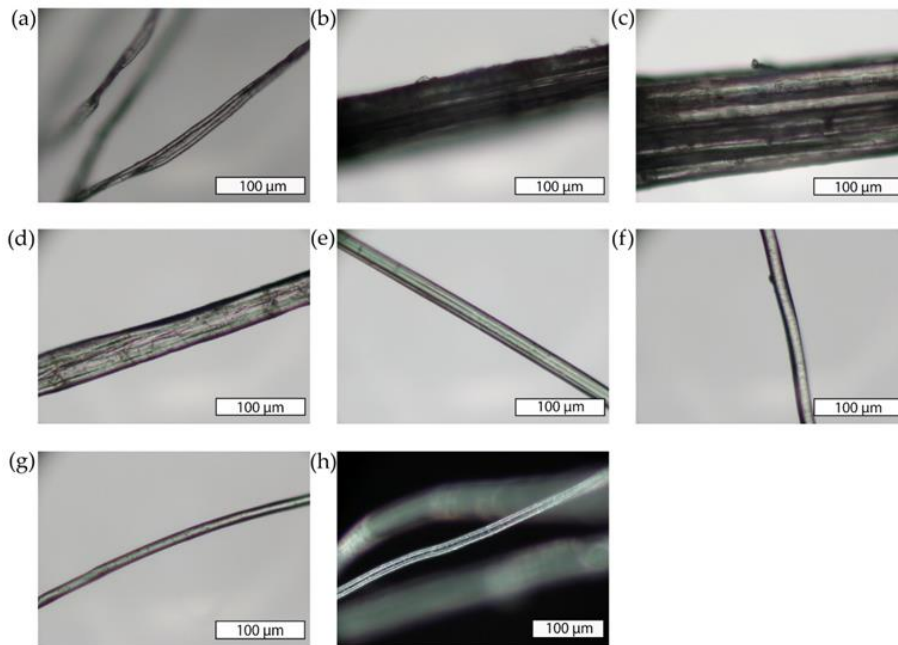


Figure 14. Images of multiple fibers, used as a reference for recognizing the microplastic fibers. natural fibers: a: cotton, b: flax, chemp, d: ramie , e: viscose , f: acrylic , g: polyester, h: polyamide eproduced from Cintron *et al.* (2024), *Microplastics*, CC BY 4.0.

Based on the visual identification criteria described above (fibers. The positions of all suspected particles were recorded in an Excel spreadsheet for further analysis. Each particle was assigned

a unique identification number along with its corresponding coordinates on the filter surface. To confirm whether the visually identified particles were microplastics, Raman spectroscopy was used as a complementary analytical technique. Before describing the Raman analysis procedure in detail, a brief overview of the Raman microscope and its application in microplastic identification is provided. Raman microscopy is a non-destructive vibrational spectroscopic technique that enables chemical characterization of materials based on the inelastic scattering of monochromatic laser light. When a laser beam interacts with a material, most photons are elastically scattered, while a small fraction undergoes energy shifts that are characteristic of the molecular bonds within the sample (**Figure 15**). These energy shifts produce a Raman spectrum that can be used as a chemical fingerprint for material identification.[60]

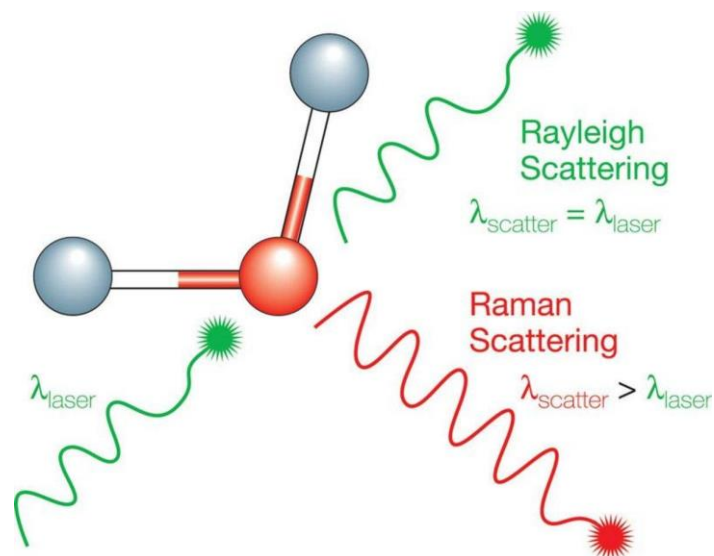


Figure 15. The scheme of Raman principle

Raman microscopy is particularly well-suited for microplastic analysis because it allows polymer identification at the micrometer scale with minimal sample preparation. Unlike some other spectroscopic techniques, Raman analysis is capable of being performed directly on particles left on filters, provided that appropriate filter materials are used. This capability makes Raman spectroscopy a widely applied method for confirming polymer types in microplastic studies, especially when combined with prior visual screening under optical microscopy [61].



Figure 16. RAMAN Microscope in the lab

In this study, Raman spectroscopy was used to chemically verify the polymeric nature of visually suspected microplastic particles identified on the polycarbonate filters (**Figure 16**). The recorded particle coordinates enabled precise relocation of individual particles under the Raman microscope, which ensured consistency between visual classification and spectroscopic confirmation.

During this stage of the analysis, several technical challenges were encountered. In order to tackle those issues, additional adjustments were required. The main challenge was the difference in coordinate systems between the Raman microscope and the digital Hirox microscope used for visual identification. This issue originated from differences in the coordinate system origins between the two instruments. To resolve this problem, a clearly distinguishable reference point was selected on each filter, and its coordinates were recorded precisely during optical microscopy. The Raman system allowed manual adjustment of the coordinate origin; therefore, after transferring the filter to the Raman microscope, the selected reference point was defined as the new origin of the Raman coordinate system. Thanks to the Raman built-in system, the origin of the device was modifiable. So, with this option, the origin was transferred to the preselected coordinate on the filter. This method enabled accurate tracking of the previously identified particles. A second challenge was related to the orientation of the

coordinate systems. Specifically, the direction of the x-axis in the Raman microscope was opposite to that of the digital microscope. As a result, coordinating the transformation was mandatory. The recorded particle coordinates were converted accordingly to ensure correct spatial alignment between the two systems. These adjustments helped us track particles more easily. Following the resolution of these technical challenges, Raman spectroscopy was applied to chemically identify the polymer composition of selected particles. The measurement parameters and data processing approach used in this study are described in the following section. Another practical challenge was related to the configuration of the Raman system itself. Indeed, the filter holder inside the microscope was not suitable for microplastic analysis, as the filters were not fixed tightly on the built-in module. Therefore, glass holders were used to place the filters securely during analysis. In addition, drawing two cross lines on the surface of the glass helped us to track particles more easily.

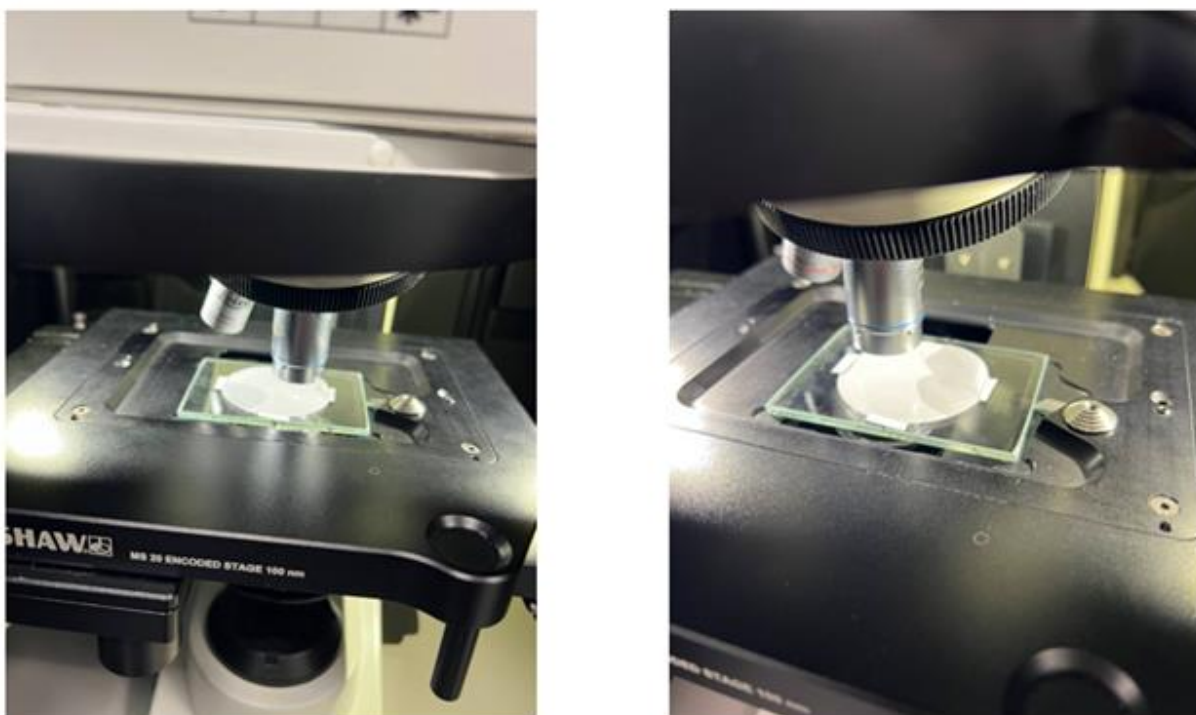


Figure 17. Customized Raman microscope configuration, proper alignment, improved stability of the filter, and facilitated accurate particle tracking during analysis.

3.7.2 Raman instrument settings

The Raman instrument settings do not remain constant during analysis. Every time due to the circumstances, an operator may modify or tweak any parameter to obtain a better signal. The most important instrument settings are: 1) laser wavelength: 785nm 2) Laser power: 1 mW to 10 mW. 3) Acquisition and integration time: ranging from 1 to seconds per frame. The table represents different parameters of the instrument in detail.

Table 6. Common Raman Parameters

| Setting | Typical Value | Purpose |
|------------------|------------------|---------------------------------|
| Laser Wavelength | 785 nm or 532 nm | Balance signal vs. fluorescence |
| Laser Power | < 10 mW | Prevent sample burning/melting |
| Objective | 50x or 100x | Focus on particles < 50 μ m |
| Integration Time | 1–5 seconds | Build a clear signal |
| Spectral Range | 100 – 3500 | Capture all polymer identifiers |

3.7.3 Raman software and spectral libraries

Raman spectra were acquired and processed using WiRE 5.7 software (build 44973) provided by Renishaw (**Figure 18**). The software was used for spectrum acquisition, baseline correction, and spectral comparison. For material identification, acquired spectra were matched against several reference libraries available within the WiRE environment.

The spectral libraries used in this study included the Renishaw Polymeric Materials Database, which contains reference spectra for a wide range of common polymer types, and the RRUFF database, primarily used for the identification of mineral and inorganic materials. In addition, a textile-specific library was employed to support the differentiation between synthetic

fibers and natural or organic fibers. A custom microplastic library, compiled from previous microplastic-related studies, was also included to improve matching accuracy for environmentally aged particles.



Figure 18. Raman analysis software and spectral libraries used in this study: WiRE 5.7 software interface for Raman data acquisition and processing

3.8 Spectral Acquisition and Data Processing

Raman spectra were obtained from each suspected particle using the instrument setting that was already defined. After relocating the particle using the coordinate, the laser was focused on the surface of the particle. In cases in which particles exhibited heterogeneous surfaces, the laser was focused on the most representative area to obtain a reliable signal. To make sure that the focused particle is the target one, each of them was completely checked with the image that was already taken by the digital microscope. The morphology, color, and homogeneity of the particles were the key apparent properties that helped us to guarantee this important issue. Background contribution originating from the filter material and the surrounding substrate was addressed by acquiring reference spectra from particle-free areas of the same filter. These background spectra were used for comparison during spectral interpretation to distinguish polymer-specific Raman peaks from signals associated with the filter or ambient noise. This approach helped reduce misinterpretation caused by substrate interference or weak background signals. It is worth noting that the spectrum of the background is generally obtained during calibration of the Raman microscope. Moreover, in some cases, the cosmic ray artifacts were

identified and removed when necessary. This was done thanks to the built-in processing tools of the Raman software. Besides, any spectra showing excessive fluorescence, unstable signals, or evidence of thermal degradation were not accepted for further analysis. The library used as references spectra was created by the lab operators themselves, claiming the most suitable library based on their experience. However, in many cases, the spectra resulting from our test were checked manually through other references, such as recently published papers. Depending on the quality of the spectra, automatic acceptance of spectra matching occurred, too. However, the confirmation could not be completely accepted until checking the signal peaks visually by the operator who oversaw the Raman device[42]. **(Figure 19)**

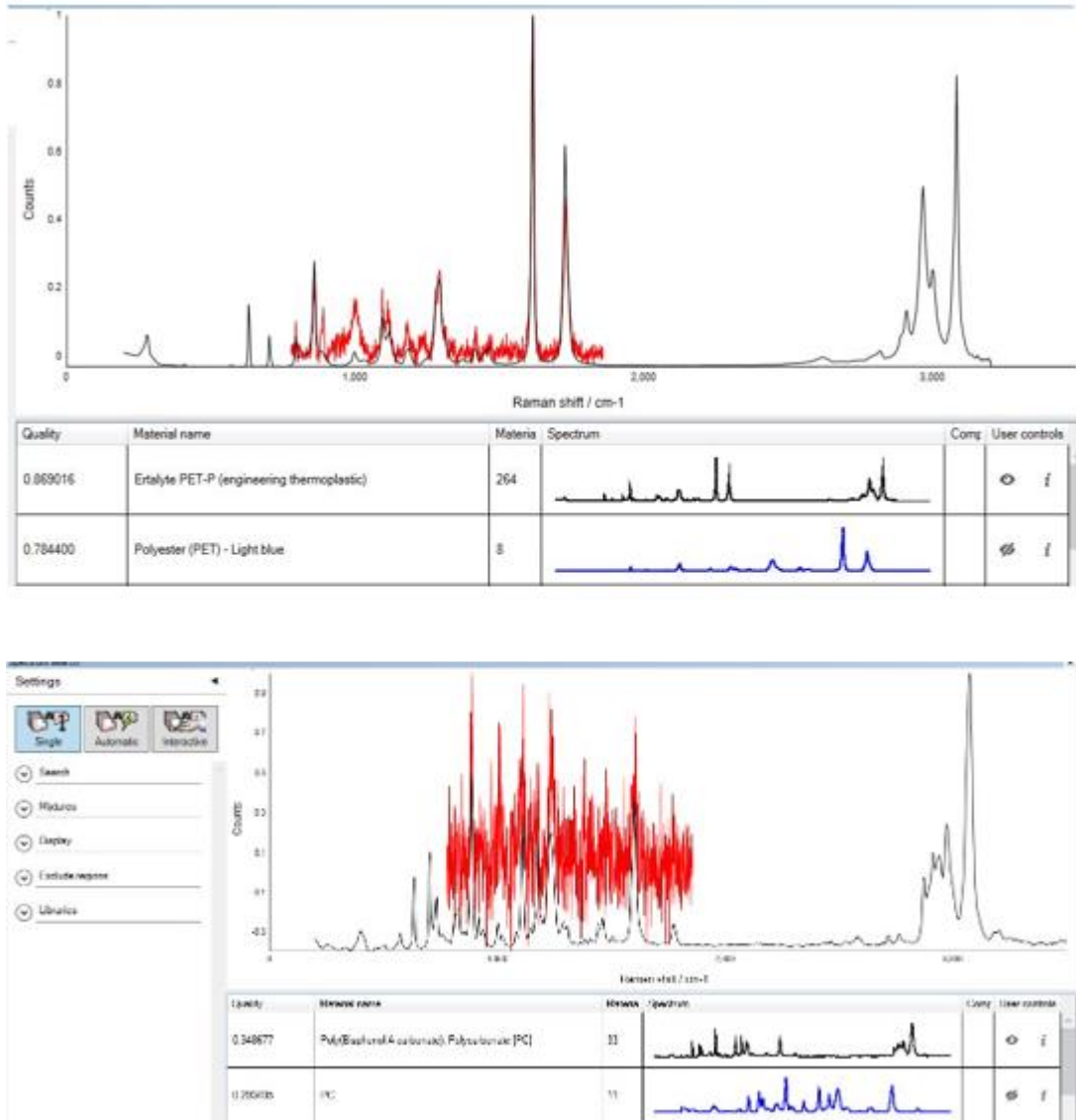


Figure 19. Raman spectra of two representative particles detected on the filtered rainfall sample, shown alongside reference spectra used for polymer identification. Top: an accepted spectrum with quality index 0.82. Bottom: no result confirmation.

3.9 Quality Control and Blank Tests

To determine potential contamination during sample preparation and tests, multiple blank tests were conducted. Five hydrogen peroxide blanks were checked to see if the samples were contaminated during the digestion step. Similarly, three ethanol blanks were tested to evaluate potential contamination from rinsing and cleaning steps. To control ambient pollution and suspended MP in the environment, six laboratory blanks were placed uncovered to be exposed to the ambient air during sample handling and measurement. Exactly the same filtration process and microscopic analysis were implemented on blank filters. This method helped us to understand and assess the possible environmental contamination that can impact microplastic quantification.

Results

4.1 Morphological and Chemical Identification of Microplastics

Microplastic fibers were found in all samples. Along with fiber microplastics, some other kinds of fibers were observed on the filter. Typical morphological characteristics of different plastics mentioned in the previous chapter helped us to distinguish microplastics from other kinds of fiber scattered on the filter (**Figure 20**). Although it is true that visual characteristics and morphological features can help identify microplastic particles, further confirmation by Raman spectroscopy is required in studies.

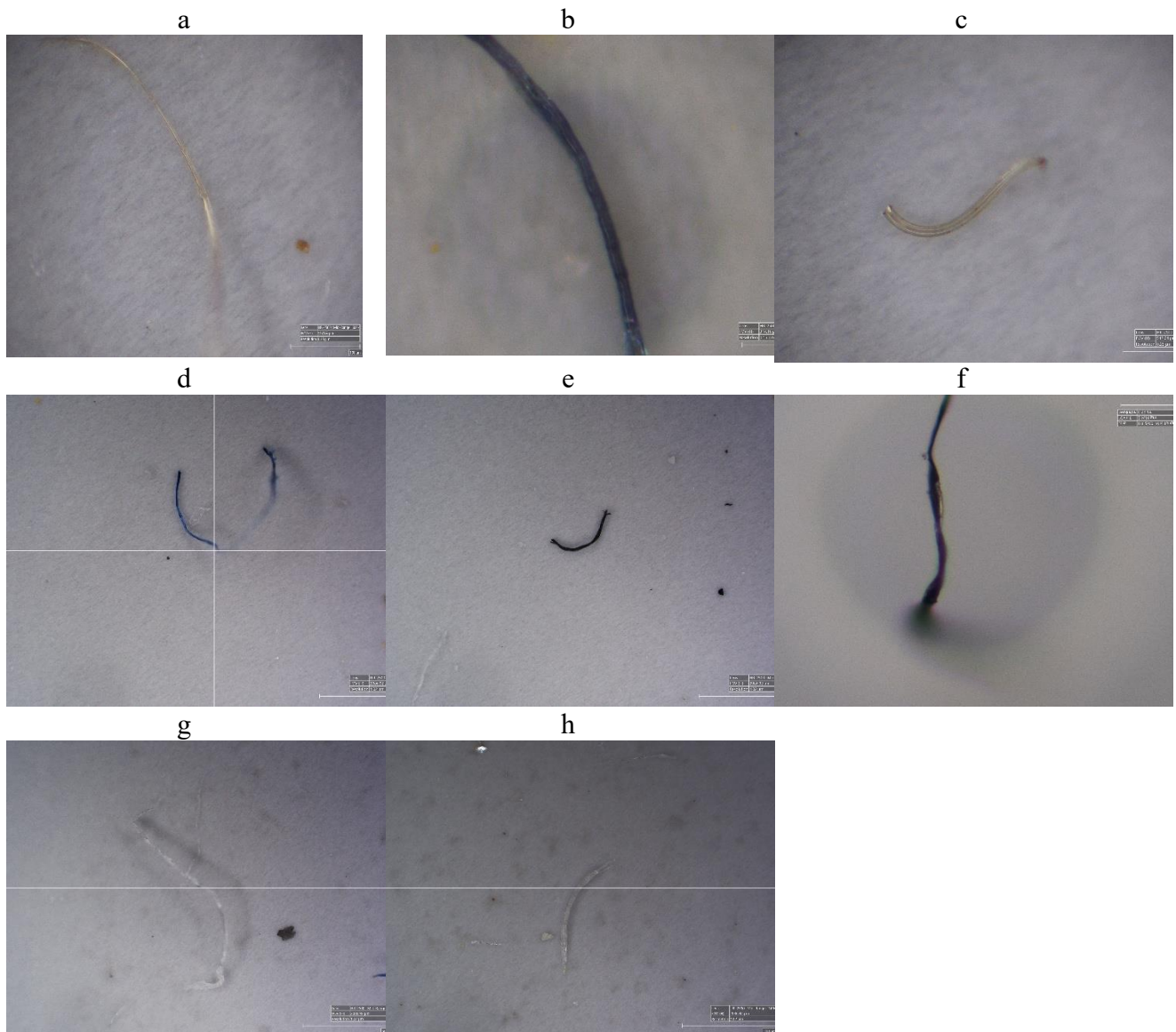


Figure 20. Representative microscopic images illustrating morphological differences between synthetic microplastic fibers (a–c), cotton fibers (d–f), and organic/natural fibers (g–h) viewed on filter membranes. Synthetic fibers almost show smooth surfaces and uniform diameters, whereas cotton fibers display twisted ribbon-like structures, and organic fibers show irregular, non-uniform morphology.

4.1.2 Raman Spectral Confirmation

Raman spectroscopy was performed to confirm the chemical composition of visually identified fibers. The resulting spectra were compared with the reference libraries. The measured spectra reflected high similarity scores, approximately 0.90, with polyethylene terephthalate (PET) reference materials. Strong peak values observed in the spectra, which align with the reference spectra, confirm the identification of the examined fibers (**Figure 21**).

Totally, 126 particles were analyzed by Raman, of which 83 were confirmed (65% accuracy).

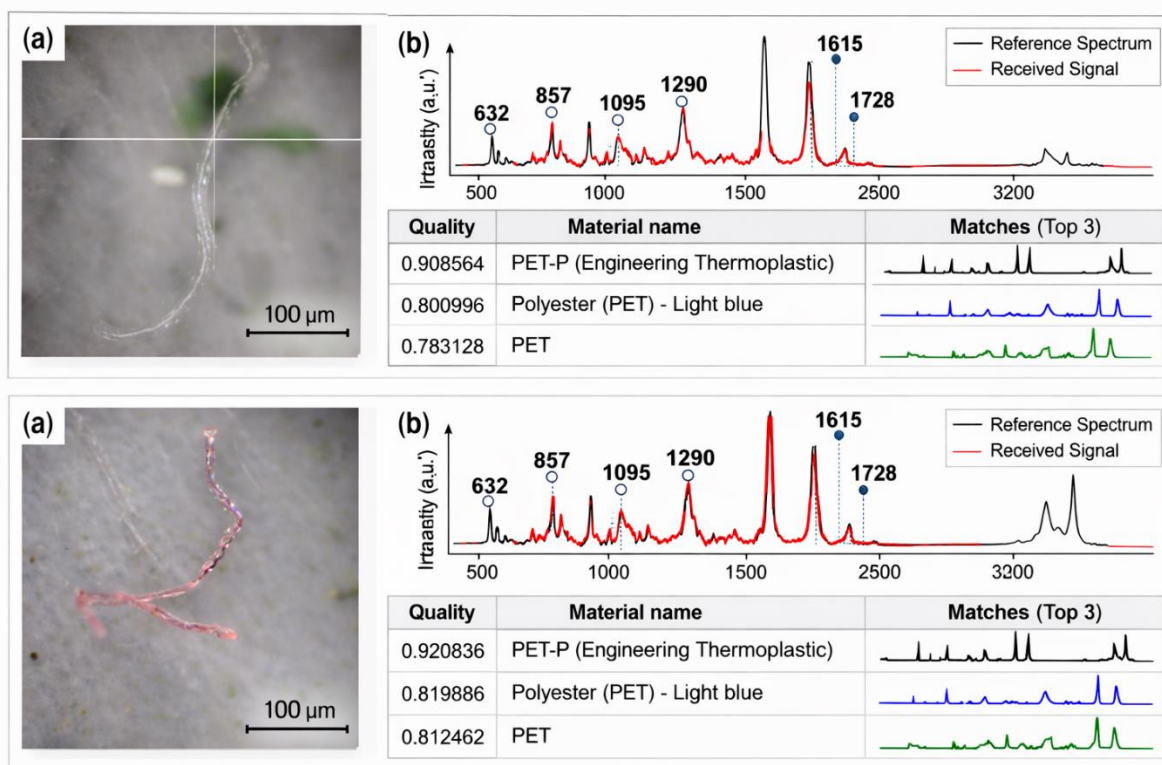


Figure 21. Up: (a) Optical image of white fiber (scale bar=100). (b) Raman spectrum of the analyzed fiber. Peaks are overlaid with the reference library spectrum. Down: (a) optical image of a pink fiber (scale bar = 100). (b): Raman spectrum overlaid with reference spectrum. The values of peaks are equal to the reference spectrum. For both fibers, the match quality is over 90 percent.

4.2 Microplastic Concentration in Rainfall Samples

All 27 samples contained microplastic fibers. The unit of concentration of MP fibers in collected rainfall is reported in particles/L. For eleven samples, the count was obtained from 12.5 percent of the filter surface, and for 16 samples, half the filter surface was extrapolated. Concentration values range from 11 to 262 particles, showing high variability among samples. (Figure 22). The mean concentration was approximately 93 particles/L, while the median was 57 particles/L, indicating slight right skew.

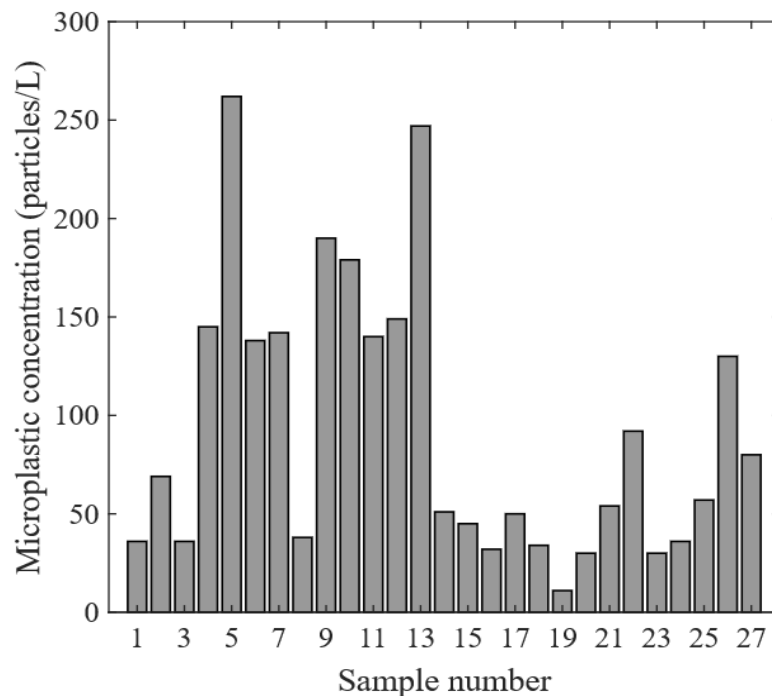


Figure 22. Microplastic concentration per rainfall sample (particles/L).

The box plot (Figure 23.a) further explains the dispersion of the dataset. The interquartile range demonstrates moderate variability. On the other hand, a few high values create an upper-tailed distribution. The histogram (Figure 23.b) shows that most sample concentration values occur within low-to-mid intervals.

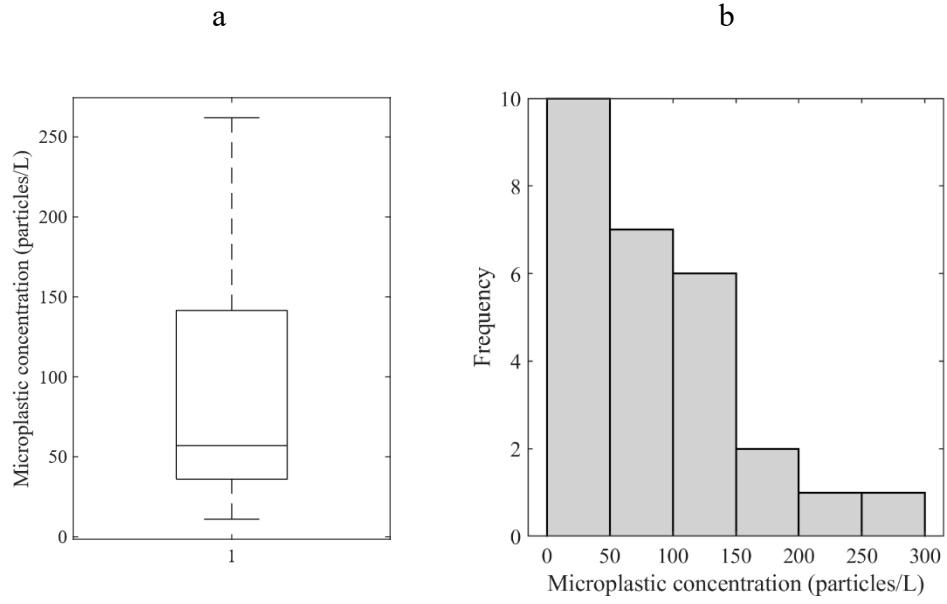


Figure 23. (a) Box plot and (b) histogram showing the distribution of microplastic concentrations (particles/L) across rainfall samples.

4.3 Morphological characteristics

4.3.1 Color distribution

A total of 189 fibers were identified. Eleven different colors were identified, indicating high variability among the colors of the fibers. The color of each fiber was carefully recorded. As shown in the figure, the white fiber was the dominant color in all samples except sample 8. The second dominant color was black. 14 samples (63%) had black fiber. Blue and gray fibers occur in most samples, but in a lower proportion. However, red, pink, purple, brown, gold, and transparent fibers were rarely observed in small numbers of samples. The highest color variety was in sample number 4, having 8 different colors at the same time. Overall, the results show that the color distribution is heterogeneous but white-dominated. (Figure 24)

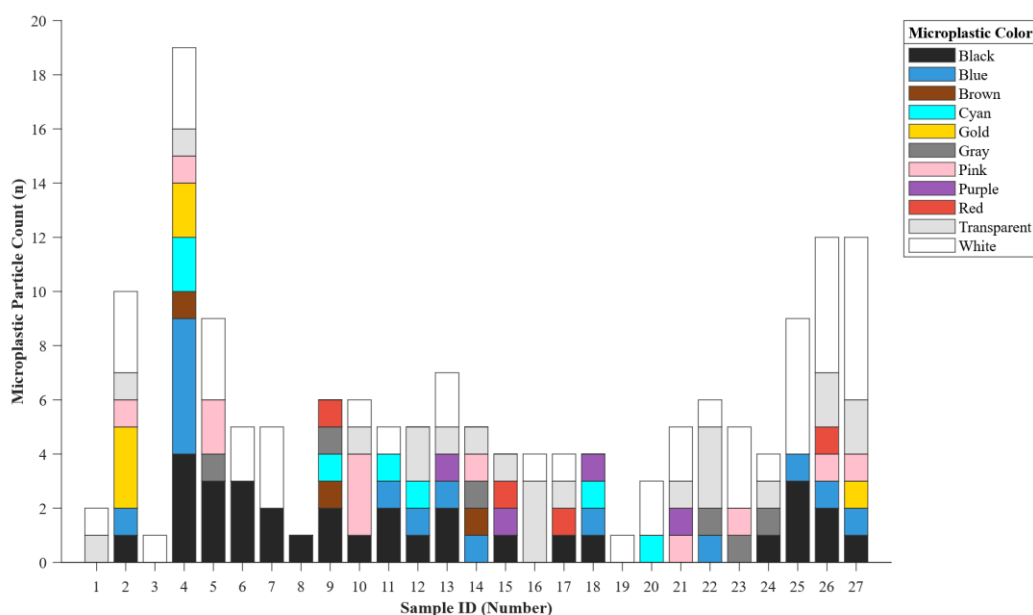


Figure 24. The number of detected fibers per color category in each sample. The maximum count belongs to white and black, respectively.

As shown in **Figure 25**, white fibers have the largest fraction (30%) of distinguished fibers, followed by black fibers. The third dominant color is transparent (14%), which shows a remarkable presence of colorless or weathered materials. All combined, neutral tones constituted roughly 64% of all detected fibers. Other colors, such as blue (9%) and pink (8%), were also present in small proportions. Similarly, colors like gray, gold, cyan, red, brown, and purple.

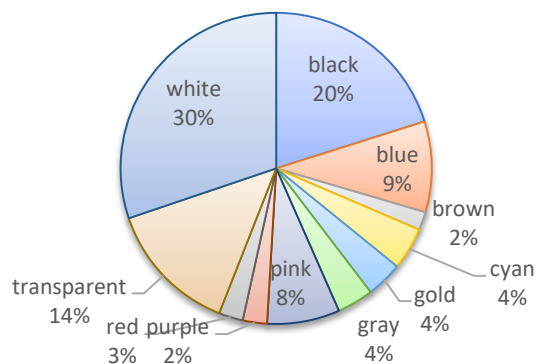


Figure 25. Overall color distribution of microplastic fibers in rainfall samples (n = 189). White (30%) and black (20%) were dominant, followed by transparent (14%) and blue (9%), while the remaining colors each accounted for <10% of total fibers.

4.3.2 UV Fluorescence Response

Among 27 rainfall samples, 18 samples (70.4%) contained fluorescent fibers during microscopic inspection. (Table 5) In total, 63 fibers were detected. Based on morphological and physical screening criteria (e.g., uniform thickness, smooth surface, and lack of natural-fiber features), 34 fibers (54.0%) were classified as suspected microplastic fibers and selected for spectroscopic confirmation. Fluorescence was used as a rapid screening indicator; however, as fluorescence may originate from dyes, additives, or organic residues, polymer identification requires Raman confirmation. [43]. As shown in **Figure 26** Fluorescence screening led to the detection of multiple fibers across the majority of samples; however, just a subset of these fibers corresponded to the morphological criteria for suspected microplastics and were then confirmed by Raman spectroscopy. It is worth mentioning that the number of fluorescent fibers varies across the filters, from 0 to 10.

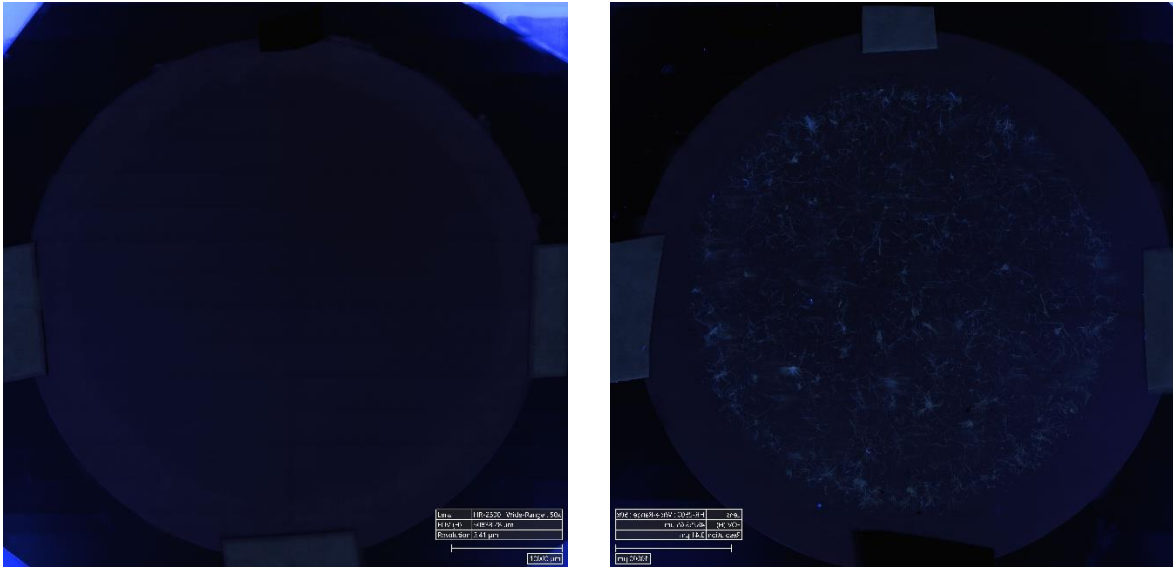


Figure 26. left: SASSO 28 filter under UV light, no fluorescent fibers. Right: SASSO 11. [Click to view the full resolution.](#)

Table 7. Summary of fluorescent fiber detection, morphological classification, and Raman confirmation in rainfall samples.

| Total Samples | Fluorescent-positive filters | Total fibers | Morphologically suspected MP | Raman confirmed |
|---------------|------------------------------|--------------|------------------------------|-----------------|
| 27 | 18 | 63 | 34 | 27 |

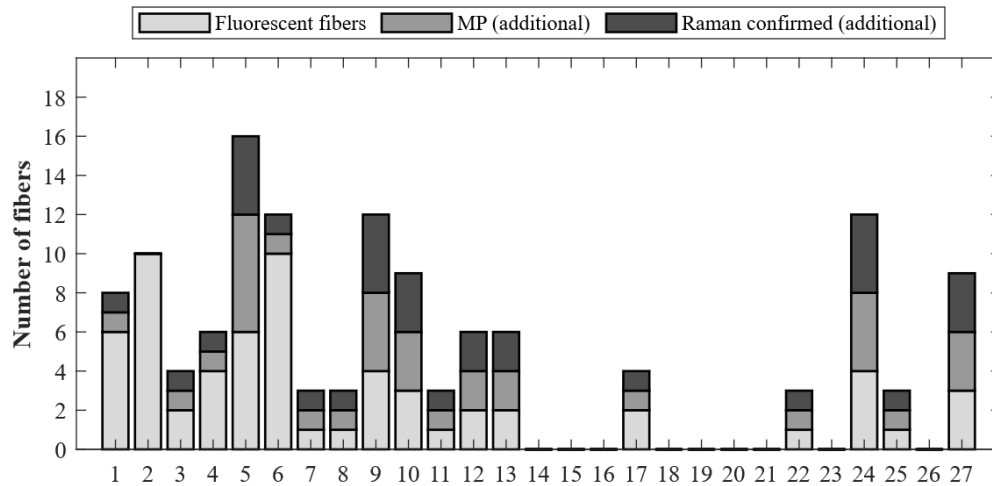


Figure 27. Stepwise identification of fibers detected in 27 rainfall samples. Fluorescence was used as an initial screening step, followed by morphological assessment to classify suspected microplastic (MP) fibers, and final confirmation by Raman spectroscopy. Bars indicate the number of fibers (n) identified at each stage for individual samples.

4.3.3 Polymer composition (Raman confirmed)

Raman analysis approved the presence of four main polymer types within the rainfall samples: PET, polyester, nylon, and acrylic. As shown in the chart (**Figure 28**), PET was detected in almost all samples. Similarly, in most samples, especially in samples 4,5,26 and 27, the same kind of fiber was the dominant one. In contrast, nylon and polyester were seen in fewer samples and in lower quantities. As shown in the pie chart (**Figure 29**), pet accounts for almost 71.4% of the total identified fibers, followed by polyester (14.3%), nylon (11%), and finally acrylic (3.2%).

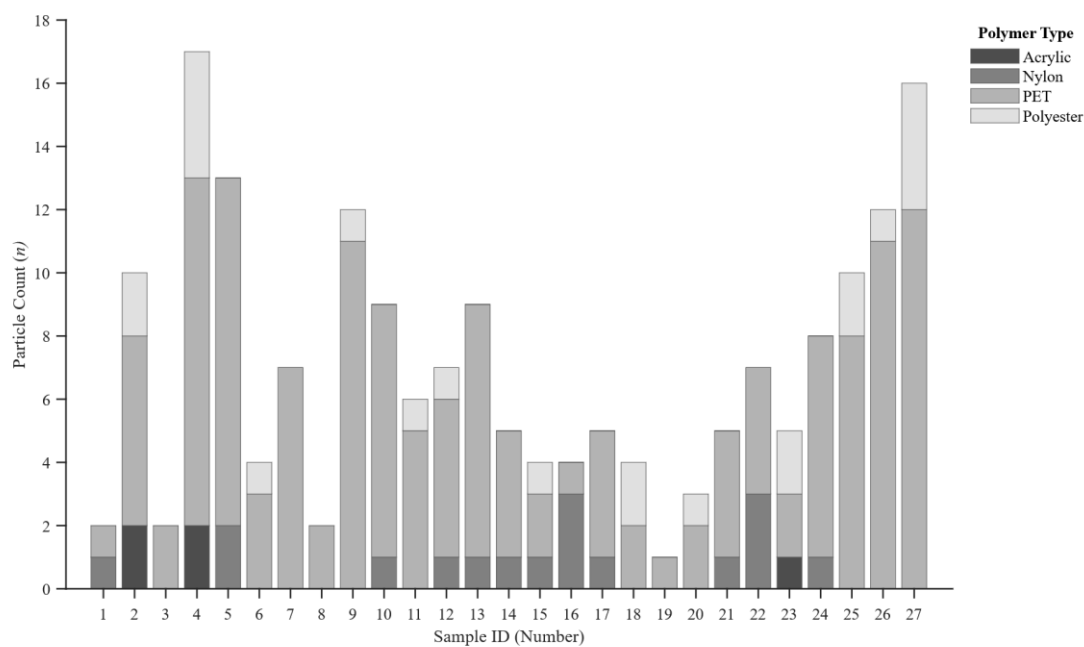


Figure 28. Polymer composition across rainfall samples. Raman-confirmed polymer counts (PET, polyester, nylon, acrylic) per sample, showing PET as the dominant type. [Click on the image to view in high resolution.](#)

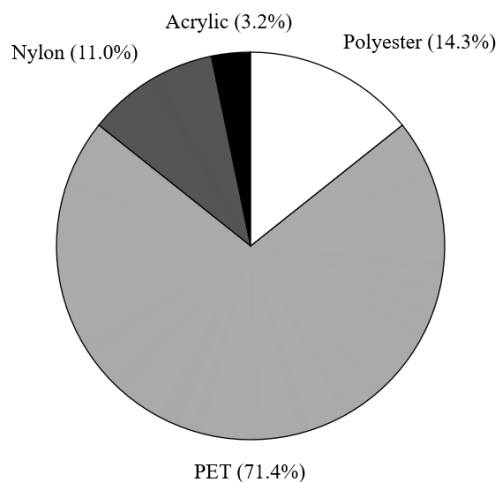


Figure 29. Overall polymer distribution in rainfall samples. (n = 189)

4.2.3 Fiber length distribution

MP fiber length ranged from 83 μm to nearly 4000 μm . The average fiber particle size is about 860 μm . As indicated in **Figure 30**, the majority of the fibers were shorter than 1000 μm . median fiber length of approximately 600–700 μm and an interquartile range roughly between 300 and 1100 μm . Several high-value outliers exceeding 2500 μm were observed, including a few fibers approaching 4000 μm (**Figure 31**). Overall, the results indicate that short fibers dominated the size distribution, while a limited number of long fibers were also present.

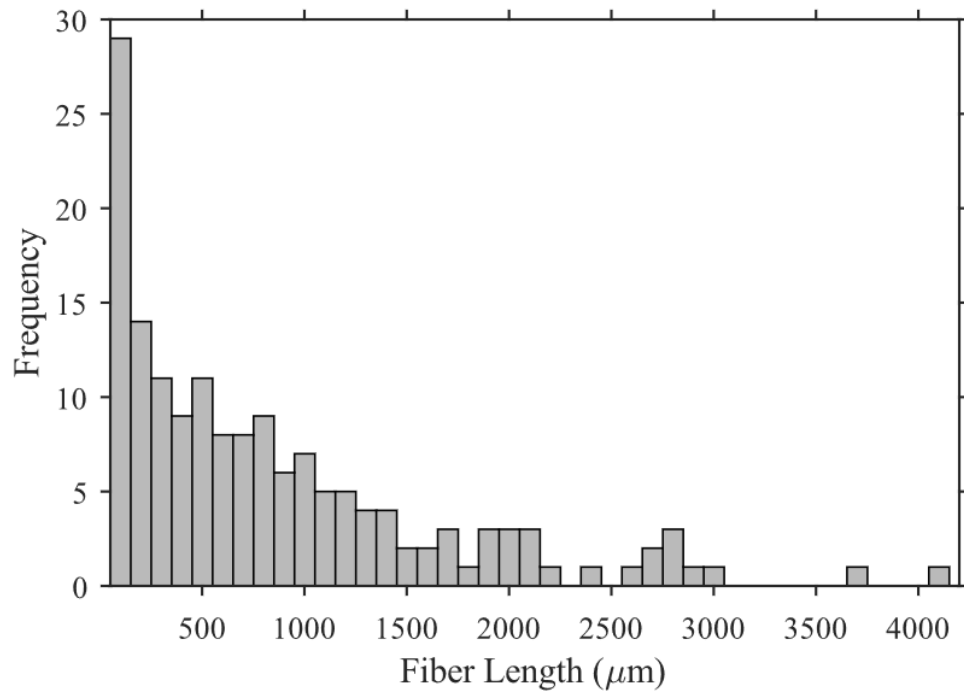


Figure 30. Frequency distribution of microplastic fiber lengths. Histogram showing a right-skewed distribution, with most fibers measuring <1000 μm and a few long-length outliers.

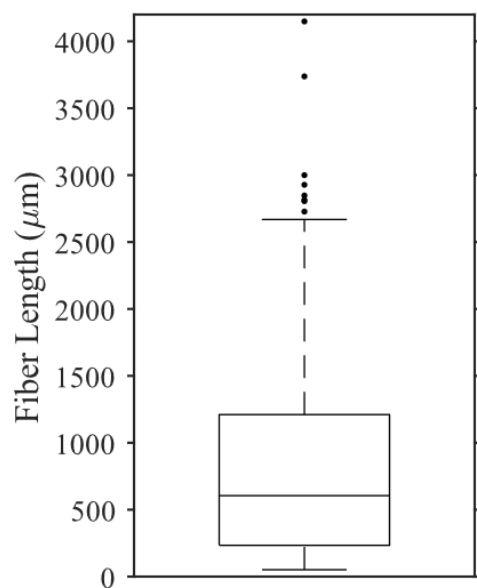


Figure 31. Statistical summary of fiber length distribution. Box plot shows median, interquartile range, and high-length outliers, confirming a positively skewed size distribution.

4.4 Blank Test Results

The hydrogen peroxide blanks showed a total of one MP particle across five tested samples. It shows minimal contamination during the digestion step. The ethanol blanks had five natural fibers in total and no confirmed MP. Laboratory airborne blanks contained seven MP across six samples. Therefore, the result set of blank tests indicates that background interference had a limited effect on the reported results.

Discussion

5.1 Microplastic Abundance and Comparison with Previous Studies

As shown earlier, the concentration of microplastic fibers in this study ranged from 11 to 200 particles/L. These quantities show a relatively elevated atmospheric deposition during precipitation in the study region. Comparing our results with those reported in some similar studies, our values are similar. For instance, in a recent study conducted in Korea[44] The concentration of MP was 91 ± 79 on average, including fragments and film. In contrast, in the present study, the focus was exclusively on fiber microplastics.

Allen et al. (2019) showed that even a remote mountainous catchment in the French Alps demonstrates high atmospheric microplastic deposition (approximately $365 \text{ particles m}^{-2} \text{ day}^{-1}$). That finding approved the fact that even in pristine environments, far from urban areas, microplastics exist. In this way, our results align with those of Allen et al. (2019).

In comparison with contamination found in the snow samples, Babaei et al. (2023) found an average abundance of 59.66 items/L in urban regions. This value is close to the median concentration of the present study.

Overall, although methodological approaches vary across studies, for instance, the morphological criteria, reporting units, sampling collection, and particle size thresholds, the concentration obtained in this study is consistent with similar studies.

In each study, depending on several factors such as the filtration process and the microscope resolution, the detection limit differs, leading to different concentration ranges.

5.2 Statistical Behavior of Microplastic Concentrations

As shown in **Figure 32**. Left: Q–Q plot of raw concentration data showing clear deviation from the reference line, indicating non-normal distribution. Right: Q–Q plot of log-transformed concentrations demonstrating improved alignment with the theoretical normal line, confirming log-normal behavior of the dataset., the concentration data followed a log-normal distribution pattern, indicating that microplastic deposition in rainfall is likely influenced by multiple interacting environmental factors rather than a single emission source. Such statistical behavior is commonly reported for atmospheric particulates and deposition-related contaminants[45].

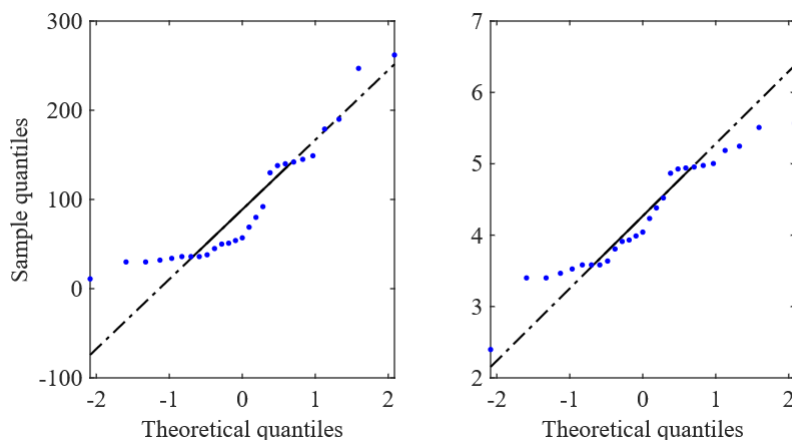


Figure 32. Left: Q–Q plot of raw concentration data showing clear deviation from the reference line, indicating non-normal distribution. Right: Q–Q plot of log-transformed concentrations demonstrating improved alignment with the theoretical normal line, confirming log-normal behavior of the dataset.

5.3 Polymer Composition and Potential Sources

Raman spectroscopy revealed that polyethylene terephthalate (PET) made up 71.4% of the analyzed rainfall samples, followed by polyester (14.3%), nylon (11%), and acrylic (3.2%). These statistics and dominance of PET are consistent with wide global production and extensive use, particularly in the synthetic textiles and packaging industries. Globally, synthetic fiber production relies heavily on polyester fibers, particularly PET, comprising over half of the total fiber manufacturing [46]. Therefore, the emergence of PET as the dominant polymer in atmospheric deposition studies seems reasonable.

Acrylic fibers represented 3.2 % of the confirmed polymers in our study. This may be because the production rate of acrylic fibers is much lower than that of polyester fibers. In addition, physical characteristics like density, along with other factors like degradation behavior and emission rate during laundering, could directly affect its atmospheric abundance. Overall, the limited detection of acrylic fiber is consistent with its lower production scale and potentially lower emission compared to PET materials [47].

5.4 Color Distribution and Environmental Implications

According to the color distribution of MP fibers, white and black were the two top dominant colors among the samples (>50%). On the other hand, colors such as red, purple, and

brown, intensely pigmented dyes, made up less than 5% of the total particles. This result was supported by similar studies that reported a predominance of neutral tones [40].

Basically, since polyester and synthetic garments are mostly produced in light or neutral shades, white fibers are usually associated with domestic and industrial textile emissions [40]. Similarly, black fiber emissions are commonly attributed to the tire wear particles and transportation systems[48].

The low abundance of strongly colored fibers can be explained by weathering. Some environmental factors, such as ultraviolet radiation, oxidation, and mechanical abrasion, can cause pigment fading [41]. Consequently, those already colored fibers appear white or transparent under microscopic scan.

5.5 Fiber length distribution and atmospheric Transport

The fiber length distribution in this study was positively skewed. The majority of fiber lengths were less than 1000 μm , and only a small quantity of long fibers were greater than 2500 μm . This right skewer pattern shows the dominance of short fibers. A small fraction of the long fibers may stand for high-value outliers. Other similar studies reported similar results in the length distribution sections. Smaller fibers tend to predominate because their physical characteristics, such as weight and aerodynamic behavior, enable them to be transported more efficiently. In detail, the presence of fibers shorter than 1000 μm and their dominance in the total indicate that fragmentation is a significant factor in shaping atmospheric MP profiles. Mechanical abrasion, ultraviolet radiation, and oxidative weathering can weaken polymer chains over time, leading to a reduction in the size of fibers [41]. Shorter fibers have the potential to remain suspended in the air for an extended period. Hence, it is more likely to be transported in remote regions through air circulation. On the other hand, the presence of larger size fibers (>2500) in our samples can be linked to local emission sources. Larger-sized fibers typically have higher settling velocities; therefore, prolonged atmospheric suspension is not likely to happen for them [49]. In conclusion, the existence of both long fibers and short fibers may be influenced by local emissions and regional atmospheric transport at the same time.

5.6 Methodological considerations

Our methodology was designed to minimize contamination and improve the reliability of the analysis, especially through Raman-based polymer confirmation. Raman spectroscopy, unlike visual identification, allows researchers to examine fibers at the molecular level. Therefore, the results of the spectral scan and subsequent identification are considered more reliable. As mentioned in previous studies, relying solely on visual criteria can put the identification at risk, since confusion with natural or organic fibers is possible during the detection of microplastic fibers. In addition, human error in visual detection may further affect the results, and any bias in classification can lead to significant errors in the outcomes. However, just like other experimental tools, Raman analysis has its own limitations, particularly fluorescence interference. Fluorescence can hide Raman signals, especially in weathered or pigmented particles, causing reduced peak resolution[50]. Sometimes polymer peaks may be entirely masked by fluorescence. Although some mitigation techniques can improve signal quality and, therefore, complete the identification process with greater reliability, fluorescence can contribute to the underrepresentation of certain polymer types.

Another variable that directly affects the quality of Raman results is the selection of optimum instrumental settings and proper operator handling. Factors such as accurate focusing and appropriate laser power selection are essential to obtain a high-quality spectrum[50]. However, determining suitable settings often requires additional time. Consequently, if more time is devoted to particle identification, the sample under analysis becomes more susceptible to contamination. For this reason, a skilled operator is essential for quickly finding the proper parameters and settings.

The color of the fibers was confirmed visually in this study. This method is highly prone to human error. It is better to use standard methods and digital software on a computer system.

6. Conclusion

The main goal of this study was to determine the contamination of microplastics in a pristine environment, such as Valle d'Aosta. Due to its geographical location, it is a suitable location to understand the domain of MP contamination and its readiness to be transported through the atmosphere. Moreover, this study sought to improve laboratory methods and address the practical challenges of identifying MP in rainfall samples, particularly by linking digital and spectroscopic microscopes.

Based on the tests and data analysis, the main conclusions are described as follows:

- A. Presence and concentration of Microplastics: Microplastic fibers existed in all 27 samples. The average concentration was approximately 93 particles/L. Statistically, the data followed a log-normal distribution, meaning that the microplastics do not come from a single source. But, their presence depends on a set of environmental factors.
- B. Polymer Types: Thanks to Raman spectroscopy, types of plastics were confirmed. Results show that PET is the most dominant polymer. It formed almost 71.4% of all confirmed polymers. This is logical, since PET is widely used globally, particularly in the textile and packaging industries. Polyester (14.3%), nylon (11.0%), and acrylic (3.2%) were also found in smaller amounts.
- C. Physical characteristics (Size and Color): the most common colors were white (30%) and Black (20%). Other colors, such as red or purple, rarely occurred in samples. This presumably happens because fibers are exposed to weathering and ultraviolet radiation during their movement in the environment.
- D. Methodological Evaluation: Raman identification accuracy was about 65%. In addition, the study proved that to detect MP fibers, visual analysis is not sufficient. Thereby, Raman spectroscopy is required to observe the molecular structure and confirm the polymer. On the other hand, Raman spectroscopy has its own limitations. During the tests, it was observed that fluorescence can mask the Raman signals, which makes it hard to identify some weathered particles. In addition, blank test results confirmed that our strict contamination prevention protocols, such as using glass jars, cotton laboratory coats, and testing blank fitters, were effective, and the results were meaningful.

7. References

- [1] T. Wang *et al.*, “Emission of primary microplastics in mainland China: Invisible but not negligible,” *Water Res.*, vol. 162, no. 5, pp. 214–224, Oct. 2019, doi: 10.1016/j.watres.2019.06.042.
- [2] R. Geyer, J. R. Jambeck, and K. L. Law, “Production, use, and fate of all plastics ever made,” *Sci. Adv.*, vol. 3, no. 7, Jul. 2017, doi: 10.1126/SCIADV.1700782;PAGE:STRING:ARTICLE/CHAPTER.
- [3] “Study reveals alarming levels of microplastic pollution in the air.” Accessed: Nov. 19, 2025. [Online]. Available: <https://www.innovationnewsnetwork.com/global-study-reveals-alarming-levels-of-microplastic-pollution-in-the-air/61800/>
- [4] S. D. Traylor, E. F. Granek, M. Duncan, and S. M. Brander, “From the ocean to our kitchen table: anthropogenic particles in the edible tissue of U.S. West Coast seafood species,” *Frontiers in Toxicology*, vol. 6, 2024, doi: 10.3389/FTOX.2024.1469995/FULL.
- [5] R. Marfella *et al.*, “Microplastics and Nanoplastics in Atheromas and Cardiovascular Events,” *New England Journal of Medicine*, vol. 390, no. 10, pp. 900–910, Mar. 2024, doi: 10.1056/NEJMOA2309822.
- [6] V. N. Prapanchan, E. Kumar, T. Subramani, U. Sathya, and P. Li, “A Global Perspective on Microplastic Occurrence in Sediments and Water with a Special Focus on Sources, Analytical Techniques, Health Risks, and Remediation Technologies,” *Water 2023, Vol. 15, Page 1987*, vol. 15, no. 11, p. 1987, May 2023, doi: 10.3390/W15111987.
- [7] “Microplastic in terrestrial ecosystems | Science.” Accessed: Jan. 29, 2026. [Online]. Available: <https://www.science.org/doi/10.1126/science.abb5979>
- [8] J. Zheng and S. Suh, “Strategies to reduce the global carbon footprint of plastics,” *Nature Climate Change 2019 9:5*, vol. 9, no. 5, pp. 374–378, Apr. 2019, doi: 10.1038/s41558-019-0459-z.
- [9] M. Carbery, W. O’Connor, and T. Palanisami, “Trophic transfer of microplastics and mixed contaminants in the marine food web and implications for human health,” *Environ. Int.*, vol. 115, pp. 400–409, Jun. 2018, doi: 10.1016/J.ENVINT.2018.03.007.
- [10] A. A. Koelmans, A. Bakir, G. A. Burton, and C. R. Janssen, “Microplastic as a Vector for Chemicals in the Aquatic Environment: Critical Review and Model-Supported

- Reinterpretation of Empirical Studies,” *Environ. Sci. Technol.*, vol. 50, no. 7, pp. 3315–3326, Apr. 2016, doi: 10.1021/ACS.EST.5B06069.
- [11] “(PDF) MICROPLASTICS IN MARINE ENVIRONMENT.” Accessed: Feb. 16, 2026. [Online]. Available: https://www.researchgate.net/publication/341411991_MICROPLASTICS_IN_MARINE_ENVIRONMENT/figures?lo=1
- [12] Q. Zhang *et al.*, “A Review of Microplastics in Table Salt, Drinking Water, and Air: Direct Human Exposure,” *Environ. Sci. Technol.*, vol. 54, no. 7, pp. 3740–3751, Apr. 2020, doi: 10.1021/ACS.EST.9B04535.
- [13] L. C. Jenner, J. M. Rotchell, R. T. Bennett, M. Cowen, V. Tentzeris, and L. R. Sadofsky, “Detection of microplastics in human lung tissue using μ FTIR spectroscopy,” *Science of The Total Environment*, vol. 831, p. 154907, Jul. 2022, doi: 10.1016/J.SCITOTENV.2022.154907.
- [14] D. C. Anih, A. K. Arowora, M. A. Abah, and K. C. Ugwuoke, “Biochemical Effects of Microplastics on Human Health: A Comprehensive Review,” 2025, doi: 10.17311/sciintl.2025.27.34.
- [15] N. Evangeliou *et al.*, “Atmospheric transport is a major pathway of microplastics to remote regions,” *Nature Communications 2020 11:1*, vol. 11, no. 1, pp. 3381-, Jul. 2020, doi: 10.1038/s41467-020-17201-9.
- [16] R. Dris *et al.*, “A first overview of textile fibers, including microplastics, in indoor and outdoor environments,” *Environmental Pollution*, vol. 221, pp. 453–458, Feb. 2017, doi: 10.1016/J.ENVPOL.2016.12.013.
- [17] S. Allen *et al.*, “Atmospheric transport and deposition of microplastics in a remote mountain catchment,” *Nat. Geosci.*, vol. 12, no. 5, pp. 339–344, May 2019, doi: 10.1038/S41561-019-0335-5.
- [18] B. Henry, K. Laitala, and I. G. Klepp, “Microfibres from apparel and home textiles: Prospects for including microplastics in environmental sustainability assessment,” *Science of the Total Environment*, vol. 652, pp. 483–494, Feb. 2019, doi: 10.1016/j.scitotenv.2018.10.166.

- [19] N. B. Hartmann *et al.*, “Are We Speaking the Same Language? Recommendations for a Definition and Categorization Framework for Plastic Debris,” *Environ. Sci. Technol.*, vol. 53, no. 3, pp. 1039–1047, Feb. 2019, doi: 10.1021/ACS.EST.8B05297.
- [20] R. C. Thompson *et al.*, “Lost at Sea: Where Is All the Plastic?,” *Science (1979)*, vol. 304, no. 5672, p. 838, May 2004, doi: 10.1126/SCIENCE.1094559;REQUESTEDJOURNAL:JOURNAL:SCIENCE;CTYPE:STRING:JOURNAL.
- [21] C. Arthur, J. E. , 1959- Baker, and H. A. Bamford, “Proceedings of the International Research Workshop on the Occurrence, Effects, and Fate of Microplastic Marine Debris, September 9-11, 2008, University of Washington Tacoma, Tacoma, WA, USA,” 2009. Accessed: Jan. 30, 2026. [Online]. Available: <http://repository.library.noaa.gov/view/noaa/2509>
- [22] K. T. Ho, R. Bjorkland, and R. M. Burgess, “Comparing the Definitions of Microplastics based on Size Range: Scientific and Policy Implications,” *Mar. Pollut. Bull.*, vol. 207, p. 116907, Oct. 2024, doi: 10.1016/J.MARPOLBUL.2024.116907.
- [23] J. Flippin, B. Murphy, and T. Tech, “Standardization of Terminology Recommendations for Microplastic Ecological Risk Assessments in the Chesapeake Bay and its Watershed PPAT Meeting,” 2020.
- [24] “Microplastics Research | US EPA.” Accessed: Jan. 30, 2026. [Online]. Available: <https://www.epa.gov/water-research/microplastics-research>
- [25] K. T. Ho, R. Bjorkland, and R. M. Burgess, “Comparing the Definitions of Microplastics based on Size Range: Scientific and Policy Implications,” *Mar. Pollut. Bull.*, vol. 207, p. 116907, Oct. 2024, doi: 10.1016/J.MARPOLBUL.2024.116907.
- [26] J. Boucher and D. Friot, “International Union for Conservation of Nature a Global Evaluation of Sources Primary Microplastics in the Oceans”.
- [27] M. Kooi and A. A. Koelmans, “Simplifying Microplastic via Continuous Probability Distributions for Size, Shape, and Density,” *Environ. Sci. Technol. Lett.*, vol. 6, no. 9, pp. 551–557, Sep. 2019, doi: 10.1021/ACS.ESTLETT.9B00379.
- [28] A. Lusher, P. Hollman, and J. Mendozal, “Microplastics in fisheries and aquaculture: status of knowledge on their occurrence and implications for aquatic organisms and

- food safety,” *FAO Fisheries and Aquaculture Technical Paper 615*, p. 147, 2017, doi: 978-92-5-109882-0.
- [29] S. Allen *et al.*, “Atmospheric transport and deposition of microplastics in a remote mountain catchment,” *Nature Geoscience 2019 12:5*, vol. 12, no. 5, pp. 339–344, Apr. 2019, doi: 10.1038/s41561-019-0335-5.
- [30] R. Dris *et al.*, “A first overview of textile fibers, including microplastics, in indoor and outdoor environments,” *Environmental Pollution*, vol. 221, pp. 453–458, Feb. 2017, doi: 10.1016/J.ENVPOL.2016.12.013.
- [31] M. Rani *et al.*, “A Complete Guide to Extraction Methods of Microplastics from Complex Environmental Matrices,” *Molecules*, vol. 28, no. 15, p. 5710, Aug. 2023, doi: 10.3390/molecules28155710.
- [32] A. Lusher, P. Hollman, and J. Mendozal, “Microplastics in fisheries and aquaculture: status of knowledge on their occurrence and implications for aquatic organisms and food safety,” *FAO Fisheries and Aquaculture Technical Paper 615*, p. 147, 2017, doi: 978-92-5-109882-0.
- [33] S. S. Monteiro and J. Pinto da Costa, “Methods for the extraction of microplastics in complex solid, water and biota samples,” *Trends in Environmental Analytical Chemistry*, vol. 33, p. e00151, Mar. 2022, doi: 10.1016/J.TEAC.2021.E00151.
- [34] J. Masura, J. E. , 1959- Baker, G. D. (Gregory D. Foster, C. Arthur, and C. Herring, “Laboratory methods for the analysis of microplastics in the marine environment : recommendations for quantifying synthetic particles in waters and sediments,” 2015. Accessed: Feb. 01, 2026. [Online]. Available: <http://repository.library.noaa.gov/view/noaa/10296>
- [35] H. LI, L. ZHU, M. MA, H. WU, L. AN, and Z. YANG, “Occurrence of microplastics in commercially sold bottled water,” *Science of The Total Environment*, vol. 867, p. 161553, Apr. 2023, doi: 10.1016/J.SCITOTENV.2023.161553.
- [36] N. M. Ashta *et al.*, “Atmospheric deposition of microplastics: a sampling and analytical method including the associated measurement uncertainties,” *Atmos. Meas. Tech.*, vol. 19, no. 2, pp. 371–388, Jan. 2026, doi: 10.5194/AMT-19-371-2026.
- [37] D. Schymanski *et al.*, “Analysis of microplastics in drinking water and other clean water samples with micro-Raman and micro-infrared spectroscopy: minimum

- requirements and best practice guidelines,” *Analytical and Bioanalytical Chemistry* 2021 413:24, vol. 413, no. 24, pp. 5969–5994, Jul. 2021, doi: 10.1007/S00216-021-03498-Y.
- [38] M. Cole, P. Lindeque, C. Halsband, and T. S. Galloway, “Microplastics as contaminants in the marine environment: A review,” *Mar. Pollut. Bull.*, vol. 62, no. 12, pp. 2588–2597, Dec. 2011, doi: 10.1016/J.MARPOLBUL.2011.09.025.
- [39] V. Hidalgo-Ruz, L. Gutow, R. C. Thompson, and M. Thiel, “Microplastics in the marine environment: A review of the methods used for identification and quantification,” *Environ. Sci. Technol.*, vol. 46, no. 6, pp. 3060–3075, Mar. 2012, doi: 10.1021/ES2031505.
- [40] R. Dris, J. Gasperi, M. Saad, C. Mirande, and B. Tassin, “Synthetic fibers in atmospheric fallout: A source of microplastics in the environment?,” *Mar. Pollut. Bull.*, vol. 104, no. 1–2, pp. 290–293, Mar. 2016, doi: 10.1016/J.MARPOLBUL.2016.01.006.
- [41] A. L. Andrady, “Microplastics in the marine environment,” *Mar. Pollut. Bull.*, vol. 62, no. 8, pp. 1596–1605, Aug. 2011, doi: 10.1016/J.MARPOLBUL.2011.05.030.
- [42] D. El Khatib *et al.*, “Assessment of filter subsampling and extrapolation for quantifying microplastics in environmental samples using Raman spectroscopy,” *Mar. Pollut. Bull.*, vol. 192, p. 115073, Jul. 2023, doi: 10.1016/J.MARPOLBUL.2023.115073.
- [43] R. Lenz, K. Enders, C. A. Stedmon, D. M. A. MacKenzie, and T. G. Nielsen, “A critical assessment of visual identification of marine microplastic using Raman spectroscopy for analysis improvement,” *Mar. Pollut. Bull.*, vol. 100, no. 1, pp. 82–91, Nov. 2015, doi: 10.1016/j.marpolbul.2015.09.026.
- [44] S. Abbasi, “Distribution of microplastics in rainfall and their control by a permeable pavement in low-impact development facility,” *J. Environ. Manage.*, vol. 351, p. 119710, Feb. 2024, doi: 10.1016/j.hazadv.2021.100035.
- [45] A. Andersson, “Mechanisms for log normal concentration distributions in the environment,” *Scientific Reports* 2021 11:1, vol. 11, no. 1, pp. 16418–, Aug. 2021, doi: 10.1038/s41598-021-96010-6.
- [46] R. Geyer, J. R. Jambeck, and K. L. Law, “Production, use, and fate of all plastics ever made,” *Sci. Adv.*, vol. 3, no. 7, p. e1700782, Jul. 2017, doi: 10.1126/sciadv.1700782.

- [47] A. Anastasopoulou, C. Mytilineou, C. J. Smith, and K. N. Papadopoulou, “Release of synthetic microplastic plastic fibres from domestic washing machines: Effects of fabric type and washing conditions,” *Mar. Pollut. Bull.*, vol. 112, no. 1–2, pp. 39–45, Nov. 2016, doi: 10.1016/j.dsr.2012.12.008.
- [48] S. L. Wright and F. J. Kelly, “Plastic and Human Health: A Micro Issue?,” *Environ. Sci. Technol.*, vol. 51, no. 12, pp. 6634–6647, Jun. 2017, doi: 10.1021/acs.est.7b00423.
- [49] S. L. Wright, J. Ulke, A. Font, K. L. A. Chan, and F. J. Kelly, “Atmospheric microplastic deposition in an urban environment and an evaluation of transport,” *Environ. Int.*, vol. 136, p. 105411, Mar. 2020, doi: 10.1016/J.ENVINT.2019.105411.
- [50] C. F. Araujo, M. M. Nolasco, A. M. P. Ribeiro, and P. J. A. Ribeiro-Claro, “Identification of microplastics using Raman spectroscopy: Latest developments and future prospects,” *Water Res.*, vol. 142, pp. 426–440, Oct. 2018, doi: 10.1016/J.WATRES.2018.05.060.